JOURNAL OF PROPULSION AND POWER
Vol. 9, No. 4, July–Aug. 1993

Research on Supersonic Combustion

F. S. Billig
Johns Hopkins University, Laurel, Maryland 20723

Introduction

SOME qualifications to the pretentious nature of the title of this Paper are in order. Research in this context is applied, i.e., it is directed toward the design and development of devices. The devices are air breathing propulsion systems, wherein supersonic combustion is inherent or it provides an adjunct benefit. Principal applications of the former are manned hypersonic aircraft, transatmospheric accelerators, and missiles. Typical examples of the latter are external burning systems that sustain thrust or reduce drag when used in tandem with primary accelerator engines.

This Paper is not at all representative of the complete body of the research on supersonic combustion. Instead, what is presented is primarily based on material with which the writer has had either direct involvement or a first-hand knowledge. It does not do justice to the exemplary works of many other investigators. Hopefully, this is somewhat rectified by the extensive list of references. The reader is encouraged to consult these manuscripts to obtain a more balanced perspective.

This applied research must be viewed from the perspective of the engineer who is charged with expediting development and is in the need of design tools. Exact physics have frequently been abandoned to produce functional models. Much of the experimental verification upon which the models are based has been obtained in facilities which have known imperfections with respect to duplication of flight conditions. Moreover, compromises have been made in the analysis and interpretation of the experimental data, in part due to imperfect or incomplete diagnostic instrumentation, and in part due to a limited understanding of the underlying physics. An example that embodies all of these deficiencies would be a design model that is based on the use of integral techniques to describe combustion in supersonic flow from experiments conducted in an arc-heated tunnel.

Beginning

When a source term for heat release is included in the energy equation and, in turn, solved simultaneously with the remaining conservation equations, the stage for supersonic combustion is set. Tsien and Beilock[1] and others,[2] having posed these equations, obtained solutions for simple diabatic flows. The mathematics certainly did not preclude supersonic initial conditions. Indeed, Pinkel and Serafini[3,4] extended the method of characteristics to include the heat source term in irrotational supersonic flow and developed a graphical solution for shock-free flow. Having established a theoretical foundation, the paramount question became, can combustion be established in steady supersonic flow? Skeptics scoffed at the possibility. "After all, flame speeds are known to be less than a few hundred feet per second, even for hydrogen-air mixtures."

Was there any solid evidence to counter the mid1950s skeptic? It was known that the speed of a traveling detonation was supersonic, relative to a stationary observer. However, a close inspection of the wave structure reveals that a strong shock precedes the heat release, thus, the initial conditions in the heat release structure of the wave front are subsonic and the final conditions are sonic, as explained by Chapman[5] and Jouget.[6] Tracer bullets fired at supersonic speeds from aircraft had been used extensively in World War II. The desired luminosity of the combustion of the solid pyrotechnic attached to the base was readily observable, but, was any of the flow in the luminous zone supersonic? (Interestingly, the "economy" intended through selectively "fueling" only a small fraction of a high-speed round was difficult to realize. The combustion reduced the base drag, thus altering the trajectory and segregating the tracer from the principal mass of the burst. It required a skilled marksman to compensate for the offset and obtain the desired lethality.) Following the war, Baker et al.[7] began to investigate wake combustion by injecting hydrogen into the base of a $2\frac{1}{4}$-in.-diam cone cylinder placed in a Mach 1.6 freejet. Similar tests were made by Scanland and Hebrank[8] who burned a solid propellant composition in the base of 40-mm projectiles. Base pressure rise due to heat release was significant in both test series, thereby substantiating the heuristic arguments that had been made to explain the alteration of the trajectory of the tracer bullets. Unfortunately, measurements to ascertain whether any part of the flame zone was supersonic were not made. The results of Davis,[9] who injected hydrogen on the base of a rearward-facing step on a flat plate at $M_0 = 1.7$, were also inconclusive. He needed to add large amounts of oxygen and/or flame holders to stabilize the combustion, which may have been confined to the subsonic wake.

The pioneering experiments of Dorsch et al.,[10–15] at the NACA Lewis Laboratories, laid to rest any lingering doubts of the veracity of combustion in supersonic flow. They had reasoned that highly reactive fuels would be needed to obtain heat release in the available residence time. Aluminum borohydride was selected for most of their work. Stable com-

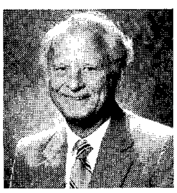

Dr. Billig is the Associate Supervisor and Chief Scientist of the Aeronautics Department of the Johns Hopkins University Applied Physics Laboratory (APL). In 1991, Dr. Billig received the lifetime achievement award from APL in recognition of his pioneering analytical and experimental contributions to the understanding and development of supersonic combustion ramjet engines, his leadership on behalf of national and international professional societies, and his decades of dedication to the education and mentoring of current and future aerospace engineers. He is a fellow, past Vice President and Director of AIAA and recipient of the 1992 Dryden Lectureship on Research presented herein.

Presented as the Dryden Lectureship on Research (Paper 92-0001) at the AIAA 30th Aerospace Sciences Meeting, Jan. 6–9, 1992, Reno, NV; received April 8, 1992; revision received Nov. 1, 1992; accepted for publication Nov. 13, 1992.

bustion, without resort to the use of physical flame holders, was demonstrated adjacent to the external surfaces on a variety of models at Mach numbers of 1.5–4.0. Computed Mach numbers based on static and pitot pressures taken within the luminous flame zone showed that the Mach number was subsonic through most of the flame zone, and became sonic and low supersonic as the hot-cold interface was approached.

These exciting results prompted the two leading institutions in ramjet development, the Johns Hopkins University Applied Physics Laboratory (JHU/APL) and the Marquardt Company, to focus attention on ramjet cycles using supersonic combustion. Nearly all of the significant research in the first several years by these organizations was not made available to the general technical community due to security classification. In recent years, permission has been granted for release of the information but, unfortunately, little has been republished. Reference 16 presents an excellent summary of the early work at Marquardt. This Paper will highlight the work at JHU/APL.

Three outstanding classified conferences on the research and application of supersonic combustion were held in the period 1959–1964. References 17–19 identify the papers that were presented, most of which should now be available. Many other authors and organizations[20–47] were also contributing to the growing body of information on the subject.

Applications

A requisite for guidance to provide focus for applied research is an appreciation of the probable applications that could exploit the results. Interestingly, the more viable concepts for the application of supersonic combustion in contemporary air breathing systems were contemplated by the pioneers in the mid-to-late 1950s. Consequently, it is appropriate to frame the discussion of the research in terms of their clairvoyant concepts. The intervening years have only provided minor modifications to the original concepts.

Applications for supersonic combustion group are divided into four major categories: 1) external burning devices for thrust production (or drag reduction) and/or lateral control; 2) primary propulsion for missiles; 3) primary propulsion for hypersonic airplanes and transatmospheric accelerators; and 4) thrust augmentation for fuel-rich rockets.

Figure 1[9] is a composite of the concepts for external burning (EB), wherein the flow in the combustion zone is supersonic. As shown, the flame zones are diffusive, whereas the original sketches of EB combustion zones[48,49] depicted a thin planar flame. The planar flame concept was a convenience to expedite simple calculations to obtain estimates of performance. From a practical perspective, it is quite doubtful that fuel could be injected in such a manner that it would mix with the air, but not ignite until reaching a prescribed plane, and then instantaneously react. Nonetheless, calculations of the required flame height in terms of model chord and the determination of engine performance as measured by specific impulse were not too different from those that would be obtained from models based on diffusion flames. The subsequent discussion will develop the arguments which show that for the same amount of heat release, performance is primarily dependent on the airflow conditions entering the combustion zone, and is only weakly affected by the character of the combustion process.

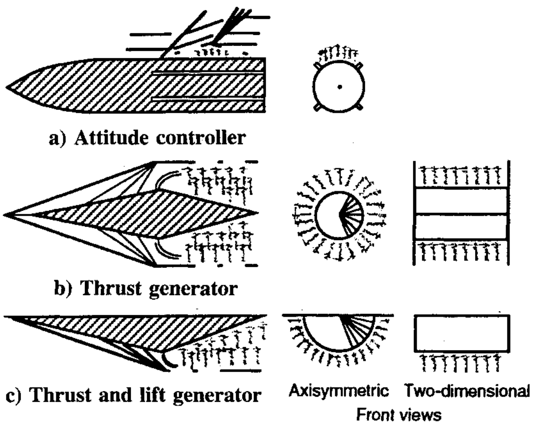

Fig. 1 External burning configurations.

In effect, EB represents a volume source which causes streamlines about the body to be deflected, giving a pressure rise similar to an aerodynamic flap, but with a significantly lesser expansion effect and no drag penalty. There is also a reaction force caused by the injection, which has components in the thrust and/or lateral directions, depending on the angle of injection. The attitude controller for an axisymmetric vehicle (Fig. 1a) has injection aft of the center-of-gravity (c.g.) in any one of four quadrants. (The periphery of the vehicle could alternatively be subdivided into any number of desired segments.) Longitudinal "fences" separate the quadrants to reduce the dissipation of the positive pressure field through circumferential spillover. The downward force due to EB leads to positive pitch (α), and therefore, puts the EB in the leeward zone, which could, at large α, produce adverse conditions for combustion. However, if EB is being used solely to trim the body, then an aerodynamically unstable vehicle could be designed, in which case the EB will always occur in the windward zone. Attitude control systems based on EB ahead of the c.g. are conceivable, but appear to be less attractive due to the difficulty of confining the positive pressure field to produce an effective pitching moment. The thrust generating device (Fig. 1b) could be either the total vehicle or a podded or airfoil engine. At the "knee," fuel is added to the air and combustion maintains a positive pressure field on the aft body which is greater than that on the compression surface, thus producing net thrust. It turns out, however, that the specific impulse decreases drastically as the EB changes from a drag-reducing to a thrust-producing device. Consequently, EB is impractical as an accelerator, and in plausible applications must be used in tandem with a primary thrust-producing device. Figure 1c bifurcates the vehicles shown in Fig. 1b, which therefore provides a combined "axial" and lateral force capability. Here, EB can provide its maximum potential. The lateral force generated by combustion negates the need for deflection of aerodynamic surfaces, and thereby eliminates induced drag with a corresponding reduction in engine fuel flow. The axial component of force due to the rise in pressure either reduces or cancels drag, and if sufficiently high levels can be obtained, then net thrust is produced.

It is advantageous to establish external combustion immediately following the forebody compression to enhance ignition in the zone of higher static temperature and pressure. Even with this assist, it is far more difficult to burn externally than within the confines of an internally ducted engine. Not only are the pressures and temperatures considerably lower in the external burner, but the residence time for completion of heat release is shorter. Moreover, if flame stabilization devices are needed, the drag penalties are much greater due to the higher dynamic pressure.

Figure 2 is taken from U.S. patent 4,291,533 awarded to G. L. Dugger and the author in 1981, following release from a long-standing "order of secrecy." This concept for a supersonic ramjet missile had been disclosed in 1959 and was reported in Ref. 50. Many interesting features are embodied in the concept. The inlet innerbody is comprised of three sections. The forward and aft sections translate, thereby adjusting the internal shock structure to obtain wave cancellation at the corners. The objective is to minimize internal losses and produce a tailored inlet compression ratio to maximize engine performance at all flight speeds. Fuel injectors are located at several axial stations to provide the variable area ratio combustion process that is desired in a scramjet engine. Many of the potential applications of vehicles powered by

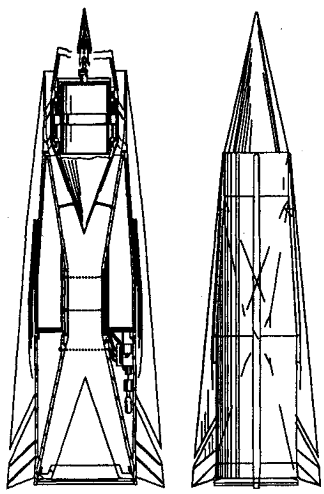

Fig. 2 Scramjet missile, U.S. patent 4,291,533, Dugger and Billig.

supersonic combustion ramjets were posed in this patent application.

> Theoretical studies have shown the possibility of propelling ramjet vehicles with hydrogen fuel to orbital speeds and with storable fuels to Mach 15 or above. . . . The margin of superiority of ramjet missiles to rockets increases rapidly as missile speed increases. To provide equivalent performance to a Mach 7 supersonic combustion ramjet vehicle at sea level, a rocket would have to have roughly three times as much weight. As an important object, therefore, the present invention provides a missile, comparable with length and volume requirements of the Terrier rocket missile system, which would accelerate from Mach 4.0 at an average of 32 g's to a cruise speed of between Mach 6.5 (7257 ft/s) and Mach 7 (7810 ft/s) at sea level, and at speeds between Mach 8.5 (8296 ft/s) and Mach 10 (9676 ft/s) at altitude.

Figure 3[51] is one of the original concepts for augmentation of the thrust of a rocket with afterburning of the fuel-rich exhaust. Air, captured in multishock inlets, is ducted into the supersonic portion of the rocket nozzle and establishes a supersonic mixing and combustion zone. The higher pressure generated in the expansion nozzle more than compensates for the drag of the air inlets, and thereby increases the net thrust of the entire vehicle. As initially proposed, the thrust augmentation would more than double the range of the solid-fueled Polaris missile. The concept was demonstrated in a liquid bipropellant (UDMH-N_2O_4) system at JHU/APL in 1963.

The fourth application is the transatmospheric accelerator, remarkably similar in concept to that of the National Aerospace Plane (NASP). In this 1959 design study,[18] the question regarding the selection of a low-speed (Mach 0–3) propulsion system was begged. The engine operated as a subsonic combustion ramjet from Mach 3 to 5, and as a scramjet from Mach 5 to 27.3. The high terminal speed permitted coasting to a low Earth orbit, with slowdown due to drag through the remaining atmosphere.

Figure 4[18b] is a schematic drawing of a sectional view of the vehicle concept. Compression was provided by a shock from the leading edge of the inlet, the convex isentropic turning surface, the cowl reflected shock, and a flame-induced shock. Properties of the inlet flowfield were obtained assuming superposition of the solutions for the inviscid and viscous portions of the flowfield. In the concept shown, a portion of the air ingested in the inlet did not participate in the combustion process, and thereby provided a film barrier to mitigate the extremely high heat transfer rates in the combustor

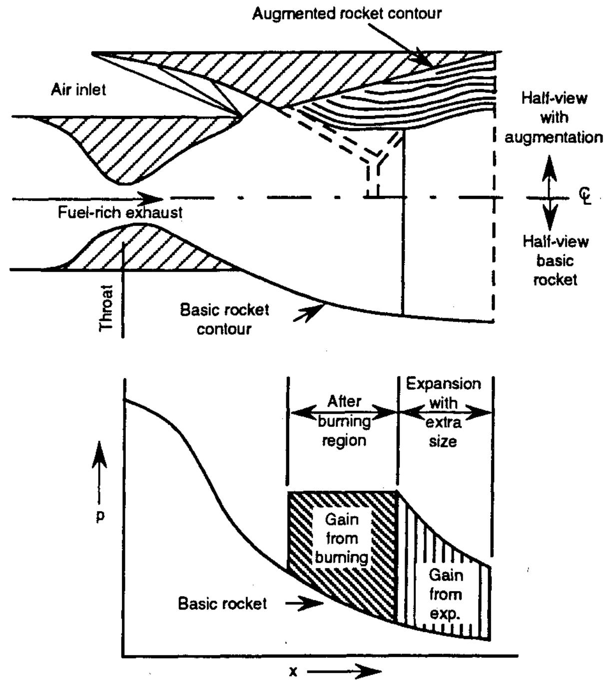

Fig. 3 Schematic illustration of air-augmented rocket.

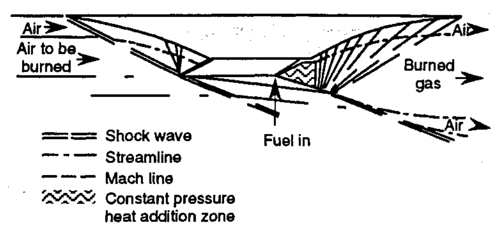

Fig. 4 Schematic of hypersonic ramjet.

and nozzle. For the cycle calculations made at that time, the flow properties were mass-averaged to obtain conditions entering the combustor. Nozzle expansions were computed for the limiting cases of frozen and equilibrium chemistry, and an assumed value of 0.33 was adopted for the nonequilibrium index. (See Ref. 52 for a discussion of nozzle loss coefficients.) The author can attest to the tedious nature of the calculations made on a mechanical desk calculator and the accompanying eyestrain from the extensive use of Mollier diagrams. Nonetheless, these calculations provided the guidance for an intensive research program at JHU/APL sponsored by NASA that began in 1961.

Interestingly, the performance estimates from 1959 are nearly identical to those that are being calculated more than 30 yr later. Moreover, several important design guidelines were recommended, as shown below.

1) Heat transferred to the vehicle must be conserved to raise the fuel to the highest allowable temperature. Therefore, convectively cooled panels are preferred over radiating surfaces, as long as the weight penalty is not too great.

2) At high hypersonic Mach numbers, the engine should be operated at a fuel-rich equivalence ratio (ER) that is larger than that required to provide adequate cooling. Typical values are ER = 1.3 at M_0 = 12, ER = 4 at M_0 = 20, and ER = 6 at M_0 = 25. High ER limits the maximum temperature in the combustion zone and thereby reduces the fraction of dissociated species in the nozzle expansion, a large-loss mechanism.

3) The fuel injection angle can be normal to the airstream at $M_0 < 10$ to enhance penetration, but must approach coaxial at high M_0. At $M_0 > 10$, the momentum of the fuel becomes an increasingly important element in the thrust potential of the engine.

4) At $M_0 \geq 20$, stored oxygen can be added to the hydrogen fuel to increase engine thrust and vehicle net force specific impulse.

5) The flight path should be suppressed to increase engine pressure to the structural limit in order to minimize nozzle nonequilibrium losses. (Dynamic pressure levels of 2000 lb_f/ft^2 and higher were recommended.)

Initial Conditions for Supersonic Combustion

For practical external burning devices, the conditions entering the combustion zone are approximately the same as they would be in the absence of combustion. In a free boundary flow about a body having a region of expansion, it is very difficult to produce additional compression by generating a flame. For a wedge airfoil such as that shown in Fig. 1, a realizable objective is to have the heat release delay the turning of the flow at the knee so that the expansion waves do not strike the airfoil. For base flows, such as behind a projectile, effective combustion would displace the expansion waves emanating from the base corner so that they fall downstream of the point of wake closure. However, for bodies that do not have an expansion region, flame compression can be generated, but the zone of higher pressure is of limited extent. A wedge-like flame zone can be established where the effective "wedge angle" corresponds to the turning angle that would cause separation of the upstream boundary layer. An example would be combustion on a flat plate aligned with the flow.[53] In summary, the initial conditions for EB lie between those in the undisturbed freestream and those that correspond to a few degrees of supersonic turning.

Conversely, in the other cited applications, the combustion is confined in a duct and the heat release can produce an upstream shock compression and thereby significantly change the initial conditions. To explain this effect, consider the flowfield in the ramjet-scramjet engine shown in Fig. 5. In the inlet the pressure increases from the freestream, P_0 to P_1, across the forebody shock and to P_3 through further turning on the external compression surface. The cowl reflected waves raise the pressure to P_4 at the entrance to the through-duct. The zone from 4 to s contains the precombustion shock structure, wherein the pressure rises from P_4 to P_s. The section of duct which confines the shock train to prevent undesirable combustor-inlet interactions is called an isolator. In the absence of combustion this shock train is not present. The strength of the shock train is determined by the amount of heat release and the effective area ratio A_5/A_4 of the combustor and, in turn, whether or not the flow at station 5 is thermally "choked." At $M_0 > 8$ the heat release is not sufficient to choke the flow, precombustion shock train disappears, and the pressure distribution in the combustor is similar to a free boundary flow. When initial conditions are considered, both those corresponding to 4 and s are pertinent. For ignition or engine relight, the shock structure would not be established, thus the initial condition is 4. Once burning is established, s is the initial condition. The pressure decreases from s to 5 in the combustion chamber and from 5 to 6 in the exhaust nozzle.

To limit the discussion, climb conditions along the flight path of a transatmospheric accelerator suffice for applications 1, 3, and 4. For air breathing missiles, the operating envelope of a Mach 3–8 surface-launched vehicle will be taken. For the former, the trajectories from Ref. 54 which temper the benefits of optimal energy management with the limitations imposed by active cooling, flutter, and sonic boom are used. For the latter, a lower altitude bound is based on heating and load limits for a passively cooled structure. The upper bound is set by minimum pressure in the combustor.

Figure 6 shows the trajectories for the transatmospheric accelerator. Takeoff is at 500 ft/s and the first segment to u = 1200 ft/s, Z = 24,218 ft is modeled as $Z = 2.035 \times 10^{-2} (u^2 - 500^2)$; the next segment to u = 6500 ft/s, Z = 77,938 ft is modeled as $u = 500 + 7.23 \times 10^{-3} Z + 8.85 \times 10^{-7} Z^2$. From u = 6500 ft/s to u = 14,000 ft/s, the vehicle flies at a constant dynamic pressure q = 2000 lb_f/ft^3. Above u = 14,000 ft/s, the constant q trajectory would produce excessive heat transfer, so in this segment to u = 28,865 ft/s, q is reduced and the trajectory follows $u = 39,256 + 0.6647 Z - 1.648 \times 10^{-6} Z^2$. The velocity at the terminal point for powered flight at Z = 175,000 ft is sufficient to overcome drag and reach a 100-nm circular orbit. A typical shuttle ascent trajectory is shown in Fig. 6 for reference.

To compute the mean flow conditions at station 4 in Fig. 5, modeling for the inlet compression process is introduced[54]:

Inlet contraction ratio

$$(A_0/A_4) = -3.5 + 2.17M_0 - 0.017M_0^2 \tag{1}$$

Inlet compression ratio

$$(P_4/P_0) = -8.4 + 3.5M_0 + 0.63M_0^2 \tag{2}$$

[Those familiar with the literature regarding performance estimates for scramjet-powered systems are aware that many authors have defined the inlet compression process by modeling the efficiency and one other parameter, usually M_4, h_4, or u_4. In Ref. 55, arguments are presented that the contraction ratio and the compression ratio are the more fundamental parameters. The experimental data bases and flowfield calculations which provided the formulation of Eqs. (1) and (2) have yet to be published in the open literature.]

Radiation to space from the inlet surfaces is assumed to reduce the total enthalpy by 1%. Table 1 lists the mean flow conditions in the freestream and the isolator entrance for the ducted supersonic combustion devices. Although the pressure rise in the inlet P_4/P_0 increases by a factor of 60 over the range of M_0, the static pressures at the isolator entrance only vary by a factor of 6. The static temperature in the core flow entering the combustor increases by about 200°R for a unit

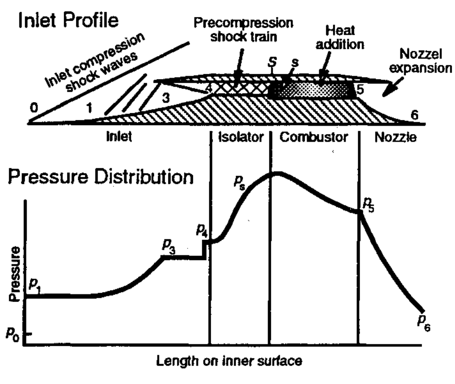

Fig. 5 Flowfield and axial-pressure distributions in a dual-mode ramjet/scramjet engine.

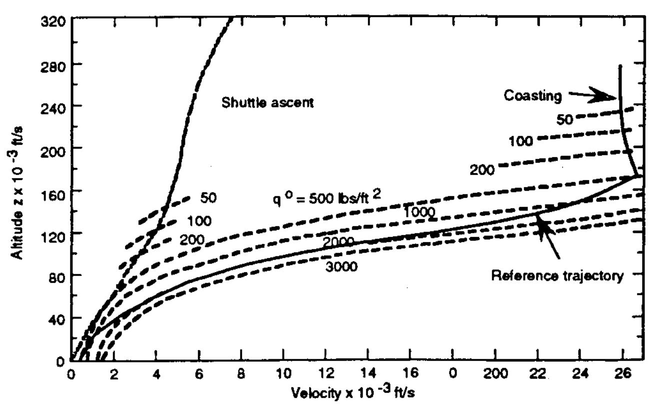

Fig. 6 Typical trajectories for transatmospheric vehicle.

Table 1 Conditions in the freestream and the combustor inlet in a typical + ram-scramjet engine[a]

Freestream conditions							Isolator entrance conditions					
M_0	Z_0, kft	p_0, psia	T_0, °R	U_0, ft/s	q_0, lb_f/ft^2	h_{t0},[b] Btu/lb_m	M_4	A_0/A_4	P_4/P_0	P_4, psia	T_4, °R	U_4, ft/s
3	47,950	1.868	390	2,904	1,694	133.3	1.529	2.86	7.8	14.51	744	2,034
4	57,480	1.183	390	3,872	1,910	264.3	1.945	4.91	15.7	18.57	930	2,885
5	65,720	7.978^{-1}	390	4,840	2,011	432.8	2.363	6.92	24.9	19.86	1,102	3,799
6	73,300	5.569^{-1}	394	5,839	2,020	646.7	2.767	8.91	35.3	19.65	1,279	4,770
7	80,077	4.049^{-1}	397.7	6,844	2,000	902.3	3.143	10.85	47	19.03	1,451	5,757
10	95,500	1.984^{-1}	406.1	9,879	2,000	1,918.2	4.143	16.49	89.6	17.78	1,958	8,744
15	114,250	8.577^{-2}	424.8	15,155	1,945	4,561.0	5.502	25.23	185.9	15.94	2,880	13,908
20	137,760	3.194^{-2}	460.8	21,040	1,287	8,824.6	6.650	33.11	313.6	10.02	4,074	19,648
26.8	178,210	6.759^{-3}	480.5	28,865	425.8	16,629.8	8.049	42.45	537.9	3.63	5,450	27,070

[a]Reference air breathing trajectory (Fig. 6). [b]$h = 0$ @ 536.7°R.

increase in M_0, and reaches a level ($T_4 > 4000$°R) where dissociation of oxygen becomes significant at about $M_0 = 19$ to 20. The values of M_4 increase monotonically with M_0, and the ratio of M_4/M_0 decreases from about 0.5 at $M_0 = 3$ to 0.3 at $M_0 = 26.8$. The velocity decrements u_0/u_4 increase from about 870 ft/s at $M_0 = 3$ to about 1785 ft/s at $M_0 = 26.8$. The velocities in the combustor remain very high at high M_0, which means that the mixing and combustion must be extremely rapid. For example, at $M_0 = 20$, the residence time in a 2-ft-long duct would be only 100 μs.

To obtain the conditions at s, modeling for ER and the combustor area ratio A_5/A_4 is needed. Those used herein were based on design studies of a single-stage-to-orbit vehicle.[54] The engine equivalence ratio for hydrogen fuel was 1 for $M_0 \leq 10$, 2 at $M_0 = 15$, 4 at $M_0 = 20$, and 6 at $M_0 = 26.8$. Below $M_0 = 5$, the shock strengths in the isolator were equal to that of normal shocks. The corresponding A_5/A_4 were 4.18 at $M_0 = 3.0$ and 2.60 at $M_0 = 4.9$. For $4.9 < M_0 < 8$, the combustor area ratios were varied from $A_5/A_4 = 1.8$ to $A_5/A_4 = 1$, to limit P_s to 125 $lb_f/in.^2$ for structural considerations. Pressure rises across the shock train for this range of M_0 correspond to those across a single oblique wave. At $M_0 = 8$, the combustor area ratio was held at unity, and P_s/P_4 decreases from about 6 at $M_0 = 8$ to about 3 at $M_0 \geq 20$.

Figure 7 shows pertinent temperatures of flows in supersonic combustors over the entire range of flight Mach numbers along the reference trajectory of Fig. 6. Static temperatures in the core flow downstream of the precombustion shock train T_s are considerably higher than the corresponding T_4 values. Nonetheless, $M_0 > 5$ is required to exceed the autoignition temperature of hydrogen. In the absence of heat release, the shock train would not be present and the autoignition condition would not be reached at $M_0 < 9$. Consequently, to assure engine relight in the event of flameout or engine unstart, an ancillary ignition source will probably have to be provided up to $M_0 = 9$. Maximum temperatures in the boundary layer can be considerably higher than in the core flow and, therefore, could provide an alternate means for ignition, but the amount of air at these elevated temperatures is small and the design of a fuel injection system that could exploit this hotter region of the flow and provide ignition would be arduous.

It should be noted that the existence of shock train structures having pressure rises P_s/P_4 greater than that required to separate an incoming boundary layer P_{sep} or, alternatively, the wisdom of designing an engine that would be operated in this mode, has been the subject of heated arguments at several technical conferences. This has been a continued puzzle to this author in that the very first tests of supersonic combustors provided conclusive evidence of the shock train structure. Moreover, the dual mode scramjet, wherein operation at $P_s > P_{sep}$ is fundamental to the concept, has been successfully demonstrated by several organizations. Aside from the controversy, failure to account for the presence of strong shock trains in analysis of engine test data leads to spurious results and erroneous solutions. In particular, unrealistically fast-mixing and heat release rates are generally deduced.

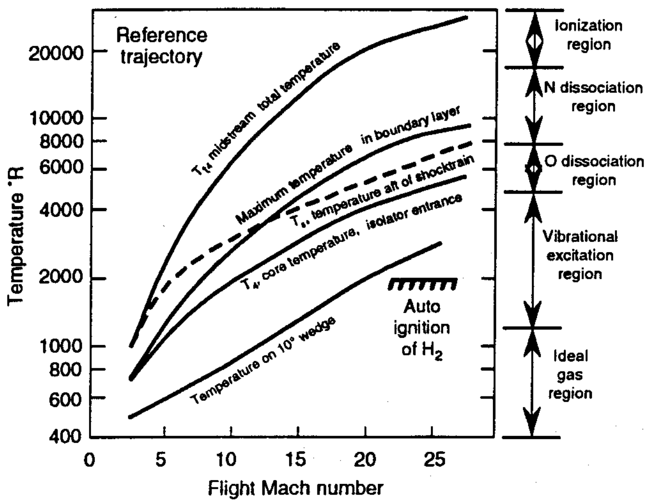

Fig. 7 Temperatures of flows entering supersonic combustors.

These comments regarding ignition of hydrogen are pertinent for hypersonic airplanes at $M_0 > 8$ and transatmospheric accelerators. Hydrogen, perhaps augmented by stored oxygen, is the only fuel that can provide the required cooling. Additives to the fuel may prove useful to either enhance ignition, accelerate the recombination reactions, and/or increase the density impulse of the fuel. For the thrust augmentation application (Fig. 3), the governing conditions regarding ignition in this "afterburning" mode of operation are those in the fuel-rich exhaust. Typical "fuel jet" Mach numbers are 2–3 with static temperatures of 2400–3200°R. Propellants are chosen that have large amounts of excess unburned hydrogen and ignition is readily obtained. For external burning systems, temperatures on a 10-deg wedge airfoil typify the initial conditions for supersonic combustion. These relatively low temperatures are a fundamental impediment to the design of a viable EB device. Hydrogen is a candidate fuel, but only with the use of flame holders whose high drag can easily negate the beneficial effects of EB. The other candidates are highly reactive liquids, e.g., aluminum, borohydride, and the aluminum alkyls or fuel-rich rocket exhausts.

Total temperatures T_{t4} are shown in Fig. 7 for reference and to provide insight to the difficult problem in producing simulated flows in ground test facilities. An even greater impediment is the corresponding total pressures which reach 5000 $lb_f/in.^2$ at $M_0 = 10$, and rapidly grow to >470,000 $lb_f/in.^2$ at $M_0 = 26.8$. Note also, that if the entire inlet compression field needed to be simulated in the ground test, the corresponding total pressures in the freestream would be >19,000 $lb_f/in.^2$ at $M_0 = 10$ and 2.4×10^7 at $M_0 = 26.8$.

Figure 8 shows the operating envelope and initial conditions for a supersonic combustion missile, such as suggested in

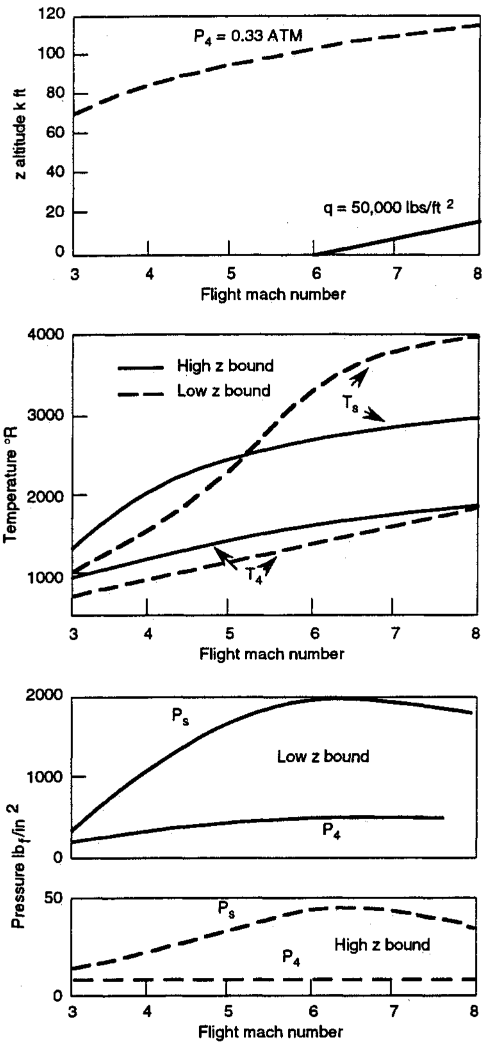

Fig. 8 Operating envelope and initial conditions for a supersonic combustion mission.

Fig. 2. The lower altitude boundary has a limiting dynamic pressure of 50,000 $lb_f/in.^2$ which corresponds to a reasonable design limit of known structural materials, passive insulators, radomes, etc. Missiles require storable fuels, which limits the available cooling capacity to flight speeds of about $M_0 = 8$. The upper bound is set by a minimum isolator inlet pressure of one-third atmosphere. Both ignition and combustion efficiency become marginal at this pressure level. For most missile applications a broad operating envelope is required, and the vehicle must be capable of both acceleration and cruise. Typically, the air breathing engine must be able to operate at flight speeds as low as $M_0 = 3$ to 4, where the temperatures T_4 are quite low. Moreover, movable parts within the supersonic combustor must either be avoided or held to a minimum. This generally prevents the use of retractable flame holders which could provide flame stabilization at low M_0, and could then be removed at high M_0, where drag and structural loads would be excessive. Indeed, these problems have been so formidable that the only successful missile concepts based on the simple scramjet cycle have required the use of highly reactive fuels.[56] Unfortunately, these fuels are logistically unsuitable for most applications. This realization prompted the invention of a hybrid scramjet at JHU/APL in 1977, known as the dual combustor ramjet, or DCR.[57,58]

It is appropriate to add a description of the DCR to complement the discussion of Figs. 1–4. A schematic illustration of the DCR concept is shown in Fig. 9. In this sketch an axisymmetric forebody serves as the initial compression surface of the supersonic inlet. In the plane of the cowl lip, the flow is subdivided into four small sectors and four large sectors. The smaller sectors direct flow to a dump-type subsonic combustor through a duct whose cross-sectional area increases with streamwise direction. This provides stable operation over a range of Mach numbers by controlling the position of the normal shock structure. These inlets are operated supercritically, i.e., the normal shock is swallowed because expulsion of the normal shock would produce detrimental interactions with the flow entering the larger flow passages.

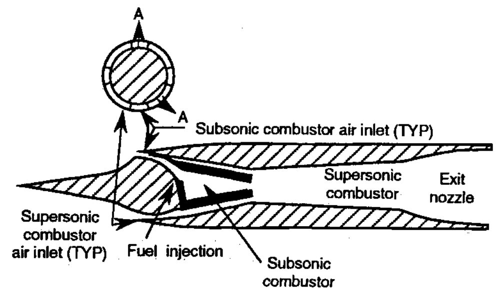

Fig. 9 Schematic illustration of dual combustor engine.

The major portion of the air is turned supersonically toward the engine axis by the outer cowl compression surface. In this design, the flow in the four ducts is spread circumferentially to form an annulus of flow in the dump plane of the subsonic combustor. The aft portion of these supply ducts is shaped so as to provide a constant or slightly increasing cross-sectional area in the streamwise direction, which serves as a combustor-inlet isolator. The shock-train structure in these ducts supports a pressure rise equivalent to a normal shock when the vehicle is operating at a high ER and low flight Mach number. For lower ER and/or higher M_0, the shock-train pressure rise corresponds to an oblique wave structure. In the "normal shock" operating mode, the mean Mach number at the combustor entrance is subsonic, and the mean Mach number in the combustor exit is either sonic or supersonic. During operation in the "oblique shock" mode, the mean flow at all stations throughout the combustor is supersonic. This gives rise to the term "dual-mode" operation, which has been discussed in considerable detail in the literature (e.g., Refs. 59–61).

The dump combustor can act as either a pilot or a gas generator to assure that heat can be efficiently released in the supersonic combustor, even when M_0 is low. If it is operated as a pilot, fuel is added to both streams; if it operated as a gas generator, all, or nearly all, of the fuel is added within it, and the main combustor becomes a supersonic "afterburner."

Research Activities

The applied research on supersonic combustion is comprised of experimental and analytical studies of "unit processes," complemented by tests and analysis of the isolator-combustor as a component or as part of an entire engine. Unit processes in this context refer to studies of shock trains, penetration of underexpanded jets, atomization of liquid jets, etc. An entire journal would be required to adequately discuss the body of material on these subjects. Instead, a selected group of the studies at JHU/APL will be described herein, and the remaining, and many of those done elsewhere, will be cited by reference. The items that are discussed are intended to 1) provide the tools to arrive at a conceptual design of a scramjet combustor; 2) present a method for simplifying and expediting computational fluid dynamics CFD analyses of flows in supersonic combustors; and 3) review experimental results to support the veracity of the modeling.

Table 2 lists the subjects that will be discussed and those that will be referenced. To keep the total list manageable, only a few representative papers from the large body of literature on computational methods (i.e., CFD) are included.

Table 2 Research items in supersonic combustion

Unit processes	References	Tests and analysis combustor or complete engine	References
Shock trains[a]	62–68	Modeling of flow structure[a]	17b, 52, 54, 58, 63, 126–129
Jet penetration	69–83	Coupling of integral and finite-difference techniques[a]	130–134
Gaseous injector design	24–90		
Shear layer mixing	19b, 24e, 29, 31, 41, 91–103	Instrumentation and data analysis	135–137
Liquid injection fuels	9, 104–112	Direct connect isolator-combustor tests and analysis[a]	16, 17c, 18b, 35, 51, 56, 60, 138–145
	9, 113–115		
Kinetics	26, 27, 52, 115–121		
Wall cooling	122–125	Free-jet engine tests[a]	58, 60, 61, 146–150

[a]Items discussed in text.

The design of an isolator combustor for a given application begins with a parametric sensitivity study using a cycle analysis code. The codes usually solve the integral form of the conservation equations for a range of initial conditions such as those given in Table 1 and Figs. 7 and 8. Engine ER and combustor area ratio A_5/A_4 are the principal variables. To solve the integral equations, the forces due to pressure and shear and the heat flux on the lateral surfaces need to be defined. The key to quantifying the pressure force is the specification of the character of the shock train. Consequently, this subject is chosen for the example of research on a unit process.

Modeling of Shock Trains

In the early days of the supersonic combustion research program, it was surmised that the shock-train structure, which had been observed in tests with fuel injection and combustion, could be duplicated in an underexpanded or throttled nonreacting flow. Moreover, it was felt that Reynolds and Mach numbers would be the fundamental correlating parameters, not pressure and temperature. Consequently, an enormously simplified test apparatus could be used. Figures 10b and 10c show two structures of shock trains in the "cold flow" test apparatus. The duct geometry duplicates the constant cross-sectional area isolator and the upstream portion of the combustor. A throttling valve is placed downstream of the step-engine combustor, shown in Fig. 10a, to simulate the blockage effects of heat release. An alternative method for generating the shock train is to lower the air supply pressure to the point where the supersonic flow at 4 is highly overexpanded. As the throttling valve is closed, a shock wave structure forms in the flow to produce the required pressure rise. At very low pressure rises, the shock structure is a series of intersecting weak waves (Fig. 10a). As the required pressure rise increases, the shocks become stronger and reach the level where the initial wave locally separates the boundary layer. If M_4 is low and the boundary layer is thick, compatibility in flow direction can only be attained with the Lambda shock structure shown in Fig. 10b. For practical engine geometries, the pressure rise on the duct walls increases monotonically over the distance S_t, but can have quite a different character in the interior of the flowfield. At high P_s/P_4 with very thick initial boundary layers or overly long isolators, the effects of viscosity change the character of the downstream portion of the interaction zone. Here, the mean flow conditions can be subsonic and the wall pressure reaches a maximum and decreases downstream.[62]

The length scales of the shock-train structure will be the basis for the engineering design tools. The overall length is denoted S_t, which is then subdivided into two parts: 1) S_0 is the length between the origin of the shock-train pressure rise and the combustor entrance, and 2) the remaining length S_d is the distance that the shock train extends into the combustor. Figure 10 has intentionally been kept simple. Actual combustors generally have far more complex injector configurations and wall geometries.

Figure 11 shows wall static pressures for a test in a cylindrical duct with an entrance Mach number $M_4 = 2.6$. Data

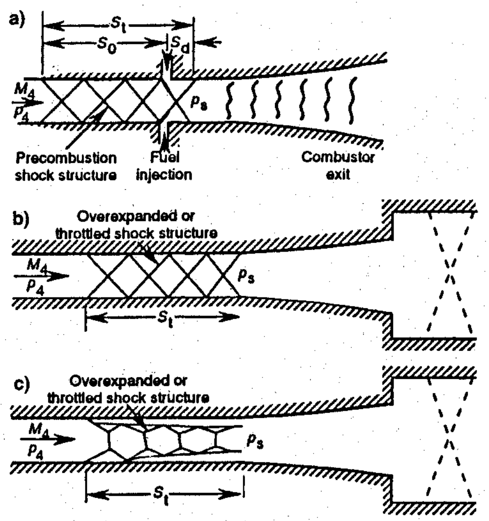

Fig. 10 Schematics of flow structure: a) isolator combustor with an oblique shock train; b) overexpanded or throttled nonreacting flow with an oblique shock train; and c) overexpanded, throttled nonreacting flow with a lambda shock train.

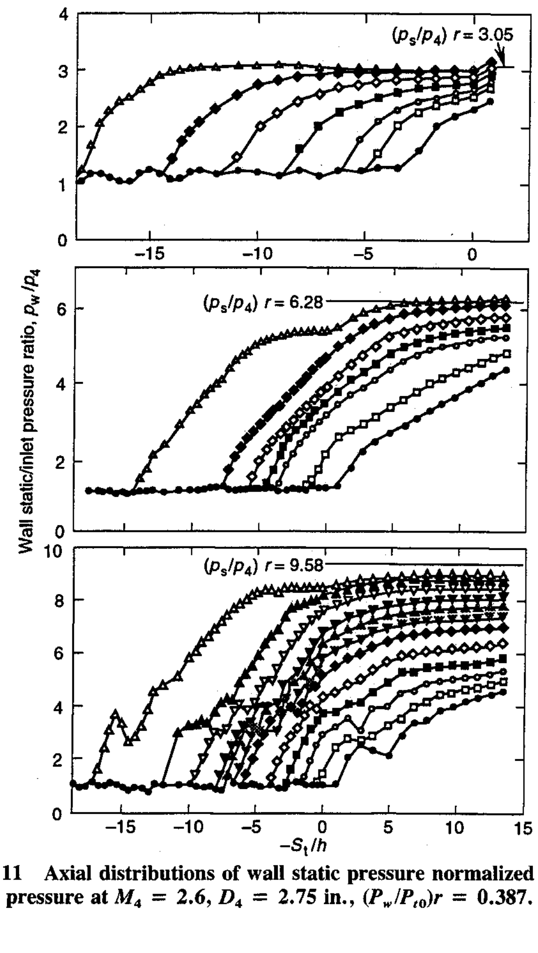

Fig. 11 Axial distributions of wall static pressure normalized to the total pressure at $M_4 = 2.6$, $D_4 = 2.75$ in., $(P_w/P_{t0})r = 0.387$.

from other cases are given in Ref. 63. In all cases, the static pressure point plotted at the duct exit station P_s, is the maximum shock-train pressure, whether it be atmospheric or that generated by throttling. The data points for the shock structures originating close to the duct exit represent the lowest value of P_s/P_4, in which some definition of the shape of the pressure rise could be made (i.e., over a 1–3-in. length). The highest data points correspond to the highest value of P_s/P_4, in which the shock train could be stabilized in the available duct length. The value of $P_w/P_{t0} = 0.34$ is somewhat lower than that corresponding to a simple normal shock, i.e., $P_w/P_{t0} = 0.42$ at $M_4 = 2.6$.

Pitot pressure measurements at radii of 0.125 and 0.375 in. from the duct centerline are shown as the solid lines in Figs. 12a and 12b. An approximate representation of the flowfield is shown in 12c, wherein the expansion fans are represented as single waves and curvature of the waves is neglected, except at points of intersection. Wave angles are constructed to yield local Mach numbers in general accord with the pitot pressure measurements, as shown by the dashed curves in Figs. 12a and 12b. These comparisons indicate that the general character of the oblique shock structure has been depicted, and that both the compression and expansion processes in reality consist of a multiplicity of oblique waves which produce continuous, rather than step changes, in P_t'/P_{t0}. Note that the interaction of the probe shock with the duct wave structure also leads to a lack of precise definition of wave locations. The calculated value of static pressure across the initial compression wave is 2.4, and the corresponding local Mach number is 1.98, which is in very close agreement with the separation criteria given by the simple modeling[151]

$$M_{sep}^2 = 0.58M_4^2 \tag{3}$$

Here, M_{sep} is the Mach number downstream of a single oblique shock, and P_{sep}/P_4 is the corresponding pressure ratio. The line depicting the boundary of the separated zone was roughly approximated from the pitot pressures.

An interesting feature—the similarity in the shape of the pressure traces—was pointed out in Ref. 63 and used as the basis for developing the engineering design model. This feature can be appreciated when all of the data for a given M_4 are superposed by shifting the origin of the pressure rise to a common point. Figure 13[63] shows the curves for the data for four values of M_4. For each set of data, the trace for a lower overall pressure rise case is simply a portion of the curve for the highest pressure rise case. Of primary interest in developing an engineering design model is the overall length of the shock train, not the details of the shape, so just the end points of the various data sets were used.

It was necessary to introduce some heuristic arguments to explore the possibility of collapsing all of the data to a single curve. The logic that was used included the following considerations:

1) For the same overall pressure rise, but a different value of M_4, the length of the structure should vary as the wavelength. Linear aerodynamic theory yields an $M_4^2 - 1$ wave-angle dependence.

2) If all other influencing factors are held constant, the flowfields should be geometrically similar; thus, S_t/D would be constant.

3) The length scale should depend on the momentum deficit in the viscous layer, and should be proportional to the total flow. Moreover, in the limit as the viscous layer approaches zero thickness, S_t should approach zero because a step rise in wall pressure could be accommodated. This situation was observed in a combustion experiment described in Ref. 144 in which the boundary layer was removed just upstream of the shock. A $(\theta/D)^N$ variation was assumed, where θ is the momentum thickness of the boundary layer, a measure of the momentum deficit. For the range of experimental data that was available, $N = \frac{1}{2}$ gave the best results.

4) The character of the boundary layer should influence the structure of the shock train, in particular, the initial separation. Thus, a Reynolds number Re dependence would be expected. As Re_θ^K increases, the boundary layer can withstand a larger P_{sep}/P_4 before separating, the initial shock angle is steeper, and S_t is smaller. The form Re_θ^K was introduced, and $K = \frac{1}{4}$ was obtained from a regression analysis of the data.

The degree of success of this approach is shown in Fig. 14, where all of the data points from Fig. 13 and Ref. 63 have

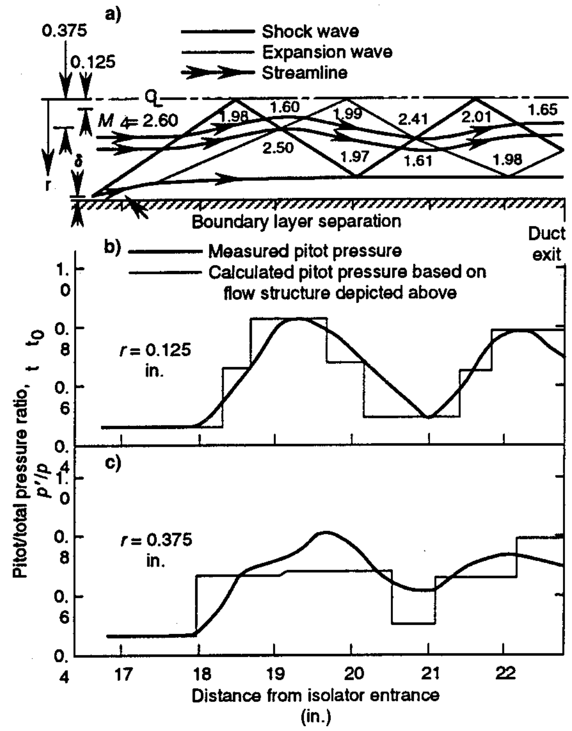

Fig. 12 Shock train structure: a) simplified representation of shock structure, b) comparison with pitot measurements at $r = 0.125$ in., c) comparison with pitot measurements at $r = 0.375$ in.

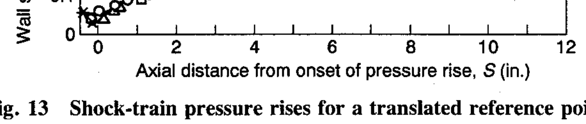

Fig. 13 Shock-train pressure rises for a translated reference point.

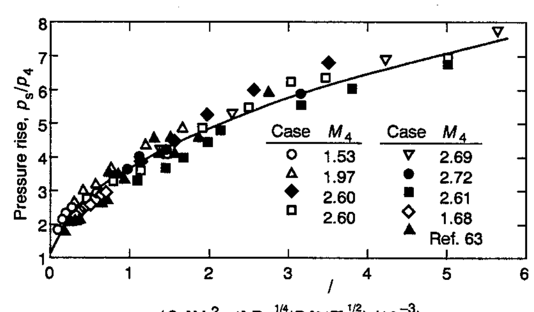

Fig. 14 Shock-train pressure rise vs correlation parameter [see Eq. (1)].

been normalized by the defined parameters. Some scatter is present, but a simple quadratic relationship

$$S_t(M_4^2 - 1)Re_\theta^{1/4}/D(\theta/D)^{1/2} = 50(P_s/P_4 - 1) + 170(P_s/P_4 - 1)^2 \qquad (4)$$

as shown by the correlation curve, is adequate for an engineering design model. Note that the empirical correlation defines not only the endpoint S_t of the pressure rise curve, but the entire wall pressure distribution, simply by replacing S_t with S and P_s/P_4 with P_w/P_4.

To apply this model to the design of the isolator and combustor, it is also necessary to locate the origin of the shock train relative to the combustor entrance, i.e., the isolator exit. For a sudden change in surface contour, such as a step between the isolator and the combustor, no ambiguity arises. For other configurations, the location of the farthest upstream fuel injector is used as the reference point for S_d (Fig. 10). The length S_d is obtained from Eq. (4) by setting $P_s/P_4 = P_{sep}/P_4$, which is the pressure ratio that will separate the boundary layer at conditions corresponding to M_4. The separation pressure ratio can be obtained from experiments or from data correlations such as Eq. (3). The minimum required isolator length S_0 is the difference between the total shock-train length and the distance the shock train extends into the combustor, $S_t - S_d$.

The invention of the dual combustor ramjet introduced a new design requirement for a combustor-inlet isolator in a coannular duct. It was necessary to determine whether the engineering design model for circular configurations would also hold for coannular configurations. A cold flow test apparatus[68] with a Mach 1–2.5 central duct flow to simulate the gas generator (Fig. 9) was used. The supersonic inlet flow was provided by annular coverging-diverging nozzles with initial Mach numbers M_4 of 1.66, 2.35, and 2.89.

The character of the pressure rise curve was similar to that of the curves for the cylindrical duct, suggesting that the shock-train structure is also similar. By simply changing the "width" scale from D to h, the duct wall separation, and translating all the shock trains to a common origin, the correlation model for the cylindrical duct gives reasonably good results for S_t (Fig. 15). The cylindrical duct model is also adequate for determining S_d when the gas generator flow is overexpanded at the point where the two jets intersect. At very high gas generator flows, however, the inner jet will tend to "pump" the annular jet and shift the shock train downstream to the point where the static pressures in the two jets match. In this flow situation, the static pressure at the discharge of the gas generator is calculated from the total pressure and the area ratio of the nozzle and is entered into Eq. (4), and the value of S calculated is set equal to S_0 to determine the anchor point of the shock train.

The extension of the engineering design model to ducts with rectangular cross sections is a topic of current study. Figure 16 shows some preliminary results from "cold flow"

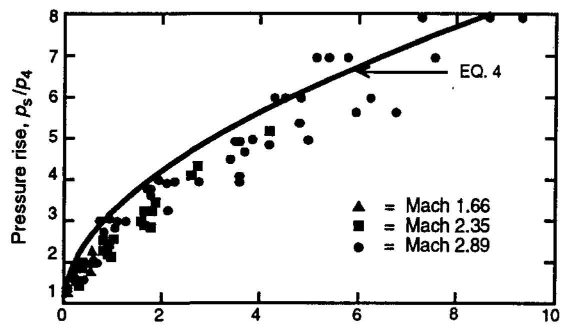

Fig. 15 Shock-train pressure distributions in coannular ducts.

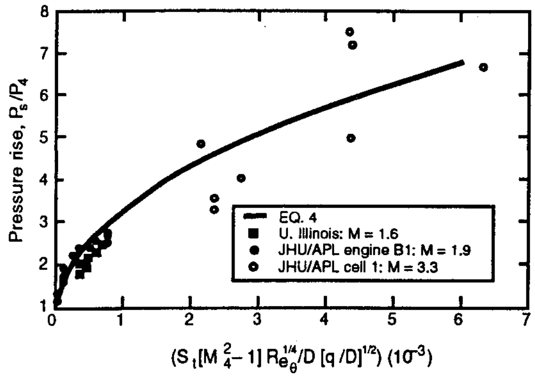

Fig. 16 Pressure rise correlation for rectangular ducts.

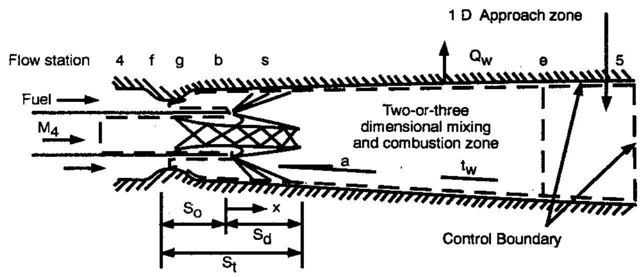

Fig. 17 Flow processes in combustor with supersonic diffusive flames.

test apparatus at the University of Illinois[64] and from direct-connect, isolator-combustor, and semifreejet engines tests at JHU/APL and the NASA Langley Research Center. Wall pressure traces were similar in character to those observed in the axisymmetric cold flow test apparatus configurations. For the data correlation in Fig. 16, the characteristic duct dimension h is taken as the smaller of the width or height of the rectangular cross section.

The boundary-layer momentum thickness at the isolator entrance is calculated or measured, and the largest θ in the centerline of a surface is used in the data correlation model. (Momentum thickness is defined as the equivalent height of inviscid duct flow that would be needed to compensate for the viscous loss of momentum in the boundary layer.) There is somewhat more scatter about the "engineering design" curve than was experienced in the axisymmetric data sets, perhaps due to the asymmetry in the viscous-inviscid interaction. Additional data and analyses are needed to determine whether modifications to the engineering design model are warranted (e.g., Ref. 67).

Modeling of the Flow Structure in a Supersonic Combustor

The model used to analyze the flow structure in supersonic combustors is shown in Fig. 17. The inflow conditions for the fuel and air are either assumed to be uniform, or are prescribed by measurements or computations of the incoming streams on the transverse upstream surfaces of the control volume. When conditions at the outflow surface, station 5, can be assumed to be uniform or approximated by defined property distributions, integral solutions for specified ER, A_5/A_4, and combustion efficiency η_c, can be obtained. Models are needed for the wall shear, heat transfer, and pressure force. If the integrated values of each of those terms are specified, then a unique solution for the downstream properties can be obtained. An infinite number of lateral wall distributions, only some of which could be physically realizable, will yield solutions. It is for this reason that entirely different modeling assumptions can yield very similar calculated outflow conditions. The challenge, however, is to devise a model which yields a plausible description of the flow structure which can then be used to define boundary conditions for finite difference solutions and, in turn, guide combustor design.

Reference 144 introduced an interesting approach to finding unique realistic solutions. The presumption is made that the flow approaching the combustor exit plane is one-dimensional, and that the wall pressure distribution in this region can be represented as the exponential

$$PA^{\varepsilon/\varepsilon-1} = \text{const} \tag{5}$$

which had first been suggested by Crocco.[152] If it is further assumed that the flow at station 5 is isentropic, then the mathematical representation for the derivatives at station 5 is

$$\left(\frac{\partial P}{\partial A}\right)_{\varepsilon=\text{const}} = [\varepsilon/(\varepsilon-1)]P/A = \left(\frac{\partial P}{\partial A}\right)_{s=\text{const}}$$

$$= [\gamma_5 M_5^2/(1 - M_5^2)]P/A \tag{6}$$

which can be rearranged as

$$M_5^2 = \varepsilon_5/[\gamma_5 + \varepsilon_5(1-\gamma_5)] \tag{7}$$

In the earlier studies that used this approach, it was assumed that the shock-train structure was confined to a constant cross-sectional area isolator. With this assumption, the wall pressure at the combustor entrance is P_s. Moreover, if the ε = constant pressure-area distribution is applied to the entire combustor wall, then the momentum equation is greatly simplified, i.e.

$$P_4A_4 - P_5A_5 + (1-\varepsilon)[P_5A_5 - (P_s/P_4)P_4A_4]$$

$$- \int_4^5 \tau_w \, dA_w = \rho_5 u_5^2 A_5 - \rho_4 u_4^2 A_4 - \rho_f u_f^2 A_f \tag{8}$$

where ρ is the density and $\rho_f u_f^2 A_f$ is the fuel momentum.

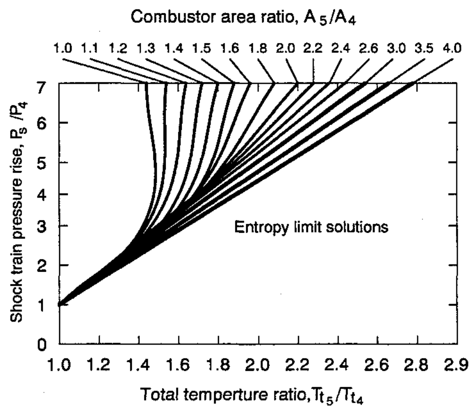

Fig. 18 Shock-train pressure rise as function of heat release (M_4 = 2.50, γ = 1.4, τ_ω = 0).

Solutions to the thereby simplified equations have served as the basis for the design of several scramjet combustors and provided considerable insight into their operating characteristics. For example, Fig. 18[59] shows the relationship between the maximum pressure rise in the shock train, P_s/P_4 and A_5/A_4, for given total temperature increases, T_{t5}/T_{t4}. The extreme sensitivity of P_s/P_4 to A_5/A_4 in these results at M_4 = 2.5 are typical for scramjets operating in the M_0 = 4 to 8 regime. The impact of this sensitivity on combustor design is immense. High P_s/P_4 is detrimental to good combustor design. It greatly increases the length requirement of the isolator and simultaneously increases the design loads. By simply increasing the combustor area at a given ER (or T_{t5}/T_{t4}), the maximum pressure rise is substantially reduced. For example, for T_{t5}/T_{t4} = 1.83 increasing A_5/A_4 from 1.4 to 2.0, decreases P_s/P_4 from 7.125, the value corresponding to a normal shock, to 4.6. The corresponding length of required isolator is reduced by a factor of 3.16. There would also be a loss in total pressure P_{t5}/P_{t4} of about 8%, but the benefits would far outweigh this loss.

When the shock train extends into the combustor to point d in Fig. 17, and the pressure area distribution in the two- or three-dimensional mixing and combustion zone, d to e, does not follow the same exponential relationship ε_5, then a more complex expression for the $\int P \, dA$ is needed. One that was suggested in Ref. 152 is

$$\int_4^5 P \, dA = KP_s(A_d - A_4) + \left(\frac{P_e + P_s}{2}\right) K_1(A_e - A_d)$$

$$+ (1 - \varepsilon_5)(P_sA_s - P_eA_e) \tag{9}$$

$$K = \int_4^5 P \, dA/P_s(A_d - A_4) \tag{10}$$

obtained from Eq. (4), and the geometry of the isolator and the portion of the combustor upstream of station d. K_1 accounts for a nonlinear pressure-area distribution in the two- to three-dimensional mixing and combustion zone. Some work has been done on the modeling of K_1 and defining the location of station e, but at present it appears that little is gained beyond the simple assumption that stations d and e are coincident and that $\varepsilon = \varepsilon_5$ over the entire region d to 5.

Although solutions to the integral equations are readily obtainable with suitable models, no information regarding the internal characteristics of the flow are forthcoming. If, however, the integral method is coupled with a finite difference method,[59,101] very useful additional information can be obtained. The procedure is outlined in Fig. 19. The first step is to solve the integral equations for the given initial conditions and combustor geometry. This yields the axial pressure distribution $P(x)$ for modeled values of wall shear τ_w and heat

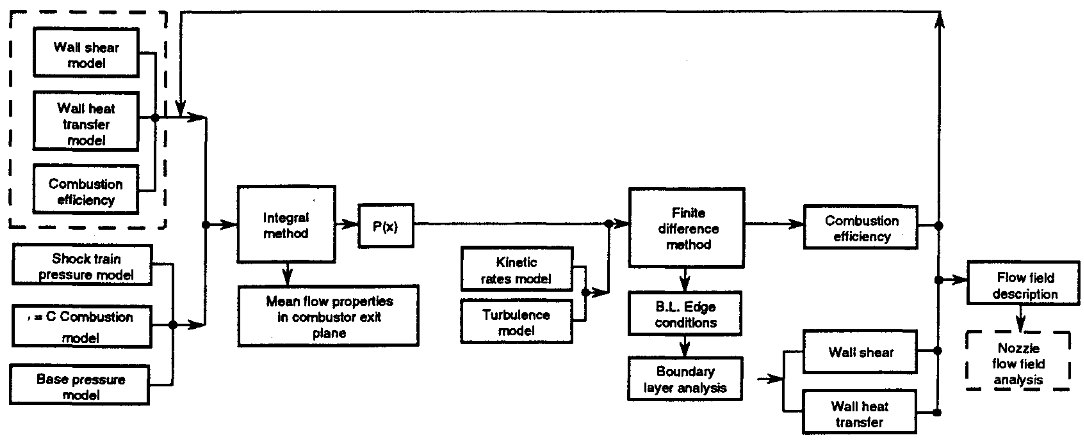

Fig. 19 Method for combining integral and finite difference methods of computation for supersonic combustor analysis.

transfer Q_w, and an assumed value for the combustion efficiency η_c. With $P(x)$ so-defined, a simplified finite-difference method that avoids calculating flow in the separated regions is made to obtain τ_w, Q_w, and η_c analytically. Inherent to the finite-difference calculations are models for kinetic rates and turbulent mixing. The integral solution is then repeated using these values of τ_w, Q_w, and η_c to obtain a new $P(x)$, etc. The iteration ends when the flow area $A(x)$, obtained from the finite-difference solution, agrees with the geometric area downstream of station s. In the region of the shock train the computed $A(x)$ generally does not match the geometric $A(x)$.

In principle, a finite-difference solution could be obtained using the geometric $A(x)$, and thereby avoid depending on $P(x)$ from the integral method. In practice, the presence of the separated zone would have to be accurately calculated, and the simplifying assumptions that permit the use of the boundary layer or parabolized forms of the Navier-Stokes equations could not be made. The form of the conservation equations would be elliptic and solutions would have to be obtained using time-dependent techniques. References 154 and 155 describe routines for such techniques that require hours of CPU time on the largest computers. Given the uncertainties that still remain in adequately describing kinetic processes, their associated rate constants, the transport properties, and the models for turbulence, the simpler, far less-expensive approach has considerable merit.

At present, solutions have been obtained that were based on the assumption that radial and circumferential pressure gradients are negligible, thereby permitting use of the boundary-layer form of the conservation equations. Additionally, it is more expeditious to first solve for the "core" flow in the combustor, iterate for $P(x)$, and then solve for the boundary layer using edge conditions from the core flow and a dense grid point spacing in the radial direction. Details of the modeling and calculated procedures are given in Refs. 59 and 129.

Whereas, there are numerous contemporary examples that establish the veracity of the foregoing modeling of combustion processes (e.g., Refs. 63 and 142), results from a few of the pioneering tests of the mid 1960s will be presented herein. Not only is this in keeping with the historical tone of this Paper, but there were some uniquely fascinating features of these tests and test apparatus.

Figure 20[144] shows the apparatus and results for a test with an inflow Mach number of 1.95. At this M_4, in an effective area ratio $A_5/A_4 = 2.27$ combustor, the heat release from an effective equivalence ratio $\mathrm{ER}_{\mathrm{eff}} = \mathrm{ER}\eta_c$ will produce a shock train having P_s/P_4 corresponding to a normal shock. In this early test, the need for, and accordingly, the provision of, an isolator was not understood. Indeed, preliminary runs that were made without the boundary-layer bleed installed were vitiated, in that the shock train invariably receded into the air supply nozzle, thereby producing poorly defined initial conditions that were atypical of those that would be expected in an actual engine. To prevent this, a boundary-layer bleed system was installed. The flow through the bleed system was governed by the local pressure in the bleed, similar to the situation that exists in the so-called "educated slot" in the inlet of an air breathing engine. The flow is proportional to the local pressure in the bleed slot. In the absence of combustion, the local pressure is low and the bleed flow is small. In the presence of combustion, the pressure is high, i.e., P_s, in this case and the bleed flow into this annular educated slot is high. With the pumping that was provided, the entire upstream boundary layer was totally removed. Thus, the shock train collapsed to a single normal shock with $S_t = 0$. This points out the possibility of reducing the length of, or eliminating an engine isolator if adequate bleed could be provided since, in accordance with Eq. (4), $\theta = 0$.

Another interesting feature of the test apparatus was the platinum gauze strips that were attached at one end to the combustor wall just downstream of the fuel injector ports. The catalytic effect on the hydrogen fuel produced ignition

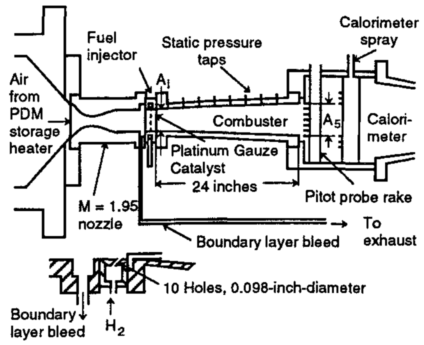

a) Schematic of hydrogen combustor test apparatus

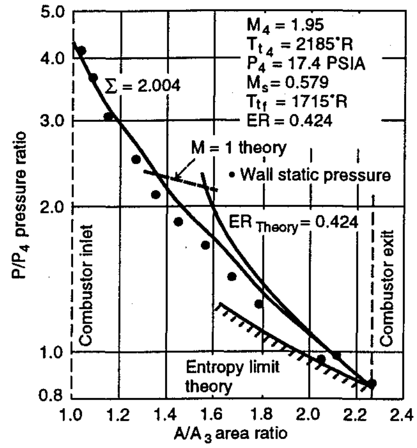

b) Combuster pressure distribution

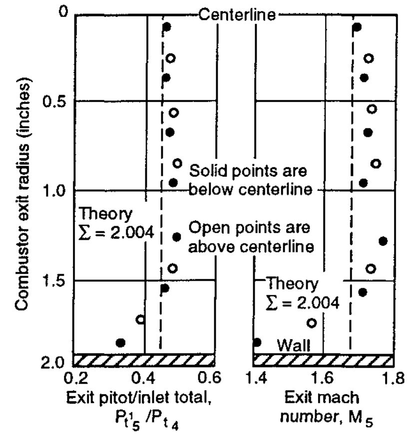

c) Combustor exit profiles

Fig. 20 Comparison of experimental and theoretical results at M_4 = 1.95.

at these relatively low temperature conditions (T_4 = 1240°R). Reference 156 discusses results of the effectiveness of a wide variety of platinum catalytic ignitors in supersonic combustors.

The wall static pressure trace for the burning runs shows the abrupt pressure rise to $P/P_4 = 4.27$, the value corresponding to a normal shock at $M_4 = 1.95$. With the removal of flow in the boundary-layer bleed, the effective area ratio of the combustor was about 10% greater than the geometric area ratio. Applying the integral method with $A_5/A_4 = 2.27$ and $\mathrm{ER}_{\mathrm{eff}} = 0.424$, and assuming the exponential pressure-area distribution holds over the entire combustor, yields $\varepsilon = 2.004$. Note the precise prediction of the exit pressure P_5/P_4 and the close correspondence between the experimental and theoretical values at the intersection of the total heat release rate and entropy limit curves. It is also of interest to note that if it is assumed that the flow has become nearly unidimensional at $A/A_4 = 1.38$, the theory would yield $M = 1$ in this plane. The lower solid curve is computed for $\varepsilon = 2.004$. The upper solid curve is the locus of end-point states (P/P_4, A/A_4) for the measured heat release. The "entropy limit" curve is the locus of end-point states for various heat release rates. The $M = 1$ curve is the locus of sonic point conditions at different P/P_4, A/A_4 values.

Figure 20c compares measured pitot pressures and local Mach numbers deduced from it with the theoretical values in the combustor exit plane. The measurements show that the core flow is near to uniform with an average value slightly in excess of the theoretical value of $M_5 = 1.67$. In retrospect, this was probably the first demonstration of the dual mode engine concept, wherein the incoming flow passed through a normal shock, became subsonic, and reaccelerated through a sonic plane to a supersonic end state.

Figure 21 shows comparison of experimental and theoretical wall pressure distributions in a combustor where the heat release produces a shock-train pressure rise that is equivalent to that of a single oblique wave. By the time this test was made (1967), the need to include an isolator in the test apparatus was clearly understood. Bulk combustion efficiencies determined from steam calorimeter measurements of the combustor exhaust gases were 0.81 and 0.92 for ER = 0.78 and 0.49, respectively. All direct-connect tests at JHU/APL use this method to determine the heat released in the combustor and, in turn, the required quantity of fuel that would have to burn to local thermodynamic equilibrium at the combustor exit. The ratio of required-to-actual fuel flow is then η_c. Gas sampling measurements from these tests and many others[142] show that η_c values less than one are generally due to lack of complete mixing. Indeed, it is difficult to conclude from measurements of hydrogen-fueled scramjet combustors having $\eta_c > 0.5$, that losses in η_c are due to slow kinetics.

	T_{t_4} (°R)	P_{t_4} (psia)	M_4	T_4 (°R)	p_4 (psia)	T_{t_f} (°R)	ER	η_c
○	4135	456	3.22	1581	7.52	1158	0.78	0.81
□	4150	456	3.22	1590	7.52	1160	0.49	0.92
◇	4150	456	3.22	1590	7.50	-	0	-

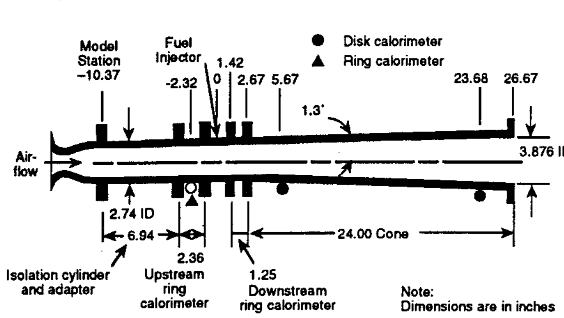

a) Schematic illustration of combustor

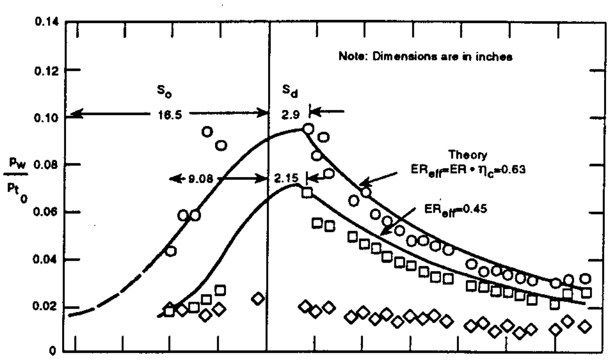

b) Pressure distribution

Fig. 21 Comparison of theoretical and experimental pressure distributions in short cyl-cone combustor at $M_4 = 3.22$.

The theoretically obtained wall pressure distributions were obtained using the shock-train modeling and again applying $\varepsilon = c$ from station s to 5. Agreement of theory and experiment is reasonably good and the general features of the flow are substantiated. Contrast this to some of the other analyses of data that have been repeated in the literature, in particular, the simple, one-dimensional method. In this method the conservation equations are solved at a finite number of axial stations in the flow, beginning at station 4. At each station the flow is assumed to have uniform properties, and any change in pressure above that due to a modeled friction and geometrical area change is attributed to heat release. In some cases, notably those with very low ER_{eff}, a plausible rate of heat release is deduced. In others, the deduced results are ridiculous. If this method was applied to the pressure distribution shown in Fig. 21, the deduced result would be that when the flow reached a station slightly downstream of s, the amount of heat released would have passed through a maximum and then would proceed to fall in the major part of the combustor. However, the final conditions in the flow would be the same as with the shock-train integral method if the values of integrated wall shear were the same. Moreover, the one-dimensional method cannot predict the wall pressure distribution for a specified ER_{eff} which is the crux of the integral model. It can only deduce the integrated value of wall pressure force.

In these tests, autoignition of the hydrogen was readily obtained. Although T_4 in the undisturbed flow was somewhat below 1800°R, the value generally required for autoignition, the strong disturbances caused by the cross-stream injection produced local zones of very high temperature. Total temperatures in these tests correspond to about $M_0 = 7.5$ flight.

The ultimate use of the modeling and analysis is the guidance it provides in engine design. The shock-train and combustor modeling that have been described played an important role in the design and development of the SCRAM engine.[56]

Figure 22 is a schematic illustration of a sectional view through one of the modules of a scramjet engine built by JHU/APL. The engine was tested in the Ordnance Aerophysics Laboratory, Daingerfield, Texas, at Mach numbers of 5 and 5.8 in 1968, and at the JHU/APL Avery Propulsion Laboratory at Mach numbers of 7–7.3 in the early 1970s. The table lists the important dimensions of the five configurations that were tested. In the taper and step configurations, the inlet was directly connected to the injector-combustor. The long isolator was designed in accordance with Eq. (4) to accommodate the strongest shock train which occurred with high ER at $M_0 = 5.8$. The shorter isolator was designed to handle shock trains at $M_0 = 7–7.3$, where the strengths were considerably lower. The tests without an isolator were made to conclusively prove the necessity of the added duct length.

Figure 23 shows the thrust coefficients for the first four configurations listed in the table on Fig. 22. The fuel in these tests was HiCal 3D, a blend of high-density liquid boranes. In the short taper configuration, the maximum thrust coef-

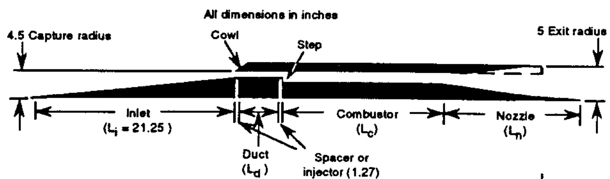

Model	L_d	L_c	L_n	Exit Nozzle	A_{ex}/A_{in}*
Taper	0.00	22.00	9.00	15° Conical	1.0000
Step	0.00	22.00	9.00	15° Conical	1.0000
Long-isolator-taper	13.50	22.00	9.00	15° Conical	1.0000
Long-isolator-step	13.50	22.00	9.00	15° Conical	1.0000
Short-isolator-step	3.50	18.25	15.00	Contoured	1.2346

* Model exit-to-inlet area ratio

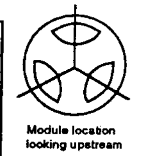

Dashed lines indicate conical nozzle
Taper—tapered combustor
Step—step combustor

Fig. 22 Schematic of APL free-jet engines.

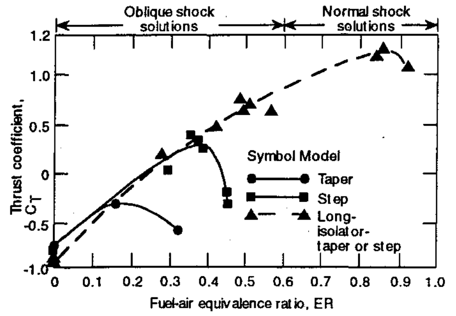

Fig. 23 Thrust coefficient of APL free-jet engine at Mach 5.0.

ficient $C_T = T/q_0A_R$, where $A_R = 78.54$ in.^{2}, occurred at ER = 0.15. Increasing the ER to 0.3 produced a region of reverse flow which was evidenced by small flame zones on the external surfaces of the engine downstream of the cowl crotches. Further increase caused a complete engine unstart and very large negative values of C_T (not shown). Putting in an abrupt step mitigated the adverse effect, moving the peak C_T to ER = 0.37. Reference 151 gives compelling arguments to show that a step permits more heat release before reaching the same P_s/P_4. With the isolator installed in either the taper or step configuration, the engine operated satisfactorily over the entire ER range. Similar satisfactory operation was demonstrated at M_0 5.8 with the long isolator and at Mach 7–7.3 with the shorter isolator. Moreover, the overall operating characteristics of the engine and the performance were in accord with that predicted by the model presented herein.

Concluding Remarks

The intent of this Paper was to show, by example, that applied research in supersonic combustion has provided the information which enables the design and development of some scramjet engines. It seems appropriate to close with a few suggested research activities to address the remaining technical issues which must be resolved to realize the full potential of the scramjet.

Mixing Enhancement

At high hypersonic speeds, the fuel (hydrogen) must have an injection angle that is close to coaxial with the air since it provides a significant portion of the exit momentum. Coaxial mixing is intolerably slow when the relative velocities of the two streams approach zero. This occurs at flight speeds of $M_0 \approx 15$, and perhaps could be called the hypersonic "pinch point." New concepts are needed to produce effective spreading angles which can be less than 1 deg at the hypersonic pinch point to required values of 3–4 deg.

Structurally Compatible Injection Systems

Most of the devices and techniques that provide good initial fuel-air distributions and/or promote mixing at moderate speeds ($M_0 < 10$) are unsuitable at high speeds. They produce local zones having extremely high-heat transfer rates. Typical examples are 1) external corners that produce vortical structures but locally thin the protective air boundary layer; 2) discrete-hole cross-stream injectors that produce strong shocks, separated flows, and reattachment zones; and 3) swept instream injectors which have excessive leading-edge heat transfer rates. Techniques that exploit the cooling capability of the fuel to protect the injectors and combustor walls while simultaneously producing the desired fuel-air distribution are needed.

Fuel Densification

The energy/unit volume of cryogenic hydrogen is so low that all-hydrogen fueled systems for many applications may not be possible (e.g., single-stage transatmospheric accelerators). The possibility of a complementary or additive component of higher density (e.g., a dense hydrocarbon, boron, boranes, etc.), appears to be attractive. Research on injection, mixing, and combustion of these bipropellant candidates in the scramjet environment is incumbent to establish feasibility.

Turbulence Modeling

It will not be possible to produce conditions in ground tests for a significant portion of the scramjet flight corridor. Consequently, computational techniques will have to be relied on for many crucial design issues. The greatest deficiency in CFD, at present, is turbulence modeling capable of predicting transition in the inlet, heat transfer, shear and mixing in the combustor, and possible relaminization in the nozzle.

References

[1]Tsien, H. S., and Beilock, M., "Heat Source in a Uniform Flow," *Journal of the Aeronautical Sciences*, Vol. 16, No. 12, 1949, p. 756.

[2]Shapiro, A. H., *The Dynamics and Thermodynamics of Compressible Fluid Flow*, Ronald Press, New York, 1953.

[3]Pinkel, I. I., and Serafini, J. S., "Graphical Method for Obtaining Flow Field in Two-Dimensional Supersonic Stream to Which Heat is Added," NACA TN 2206, Nov. 1950.

[4]Pinkel, I. I., Serafini, J. S., and Gregg, J. L., "Pressure Distribution and Aerodynamic Coefficients Associated with Heat Addition in Two-Dimensional Supersonic Wing," NACA RM E51K26, Feb. 1952.

[5]Chapman, D. L., *Philosophy Magazine*, Vol. 47, 1899, p. 90.

[6]Jouguet, E., *Mechaniques des Esplosifs*, Dorn, Paris, 1917.

[7]Baker, W. T., Davis, T., and Matthews, S. E., "Reduction of Drag of a Projectile in a Supersonic Stream by the Combustion of Hydrogen in the Turbulent Wake," Applied Physics Lab., CM-673, Johns Hopkins Univ., Laurel, MD, June 1951.

[8]Scanland, T. S., and Hebrank, W. H., "Drag Reduction Through Heat Addition to the Wake of Supersonic Missiles," Ballistic Research Lab., Memo Rept. 596, Aberdeen, MD, June 1952.

[9]Billig, F. S., "A Review of External Burning Ramjets," Applied Physics Lab., TG-801, Johns Hopkins Univ., Laurel, MD, Dec. 1965.

[10]Fletcher, E. A., Dorsch, R. G., and Gerstein, M., "Combustion of Aluminum Borohydride in a Supersonic Wind Tunnel," NACA RM E55D07a, June 1955.

[11]Dorsch, R. G., Serafini, J. S., and Fletcher, E. A., "A Preliminary Investigation of Static-Pressure Changes Associated with Combustion of Aluminum Borohydride in a Supersonic Wind Tunnel," NACA RM E55F07, Aug. 1955.

[12]Dorsch, R. G., Serafini, J. S., and Fletcher, E. A., "Exploratory Investigation of Aerodynamic Effects of External Combustion of Aluminum Borohydride in Airstream Adjacent to Flat Plate in Mach 2.46 Tunnel," NACA RM E57E16, July 1957.

[13]Dorsch, R. G., Allen, H., Jr., and Dryer, M., "Investigation of Aerodynamic Effects of External Combustion Below Flat-Plate Model in 10- by 10-foot Wind Tunnel at Mach 2.4," NASA D-282, April 1960.

[14]Serafini, J. S., Dorsch, R. G., and Fletcher, E. A., "Exploratory Investigation of Static- and Base-Pressure Increases Resulting from Combustion of Aluminum Borohydride Adjacent to Body of Revolution in Supersonic Wind Tunnel," NACA RM E57E15, Oct. 1957.

[15]Dorsch, R. G., Serafini, J. S., Fletcher, E. A., and Pinkel, I. I., "Experimental Investigation of Aerodynamic Effects of External Combustion in Airstream Below Two-Dimensional Supersonic Wing at Mach 2.5 and 3.0," NASA 1-11-59E, March 1959.

[16]Krull, H. G., Bahn, G. S., Kushida, R., Fisher, R. E., and Koffer, G. W., "Final Summary Report. Investigation of Supersonic Burning for the Period 1 March 1957 to 31 July 1958," Marquardt Aircraft Co., Van Nuys, CA, Aug. 1958.

[17]Selected Papers, Second Symposium on Advanced Propulsion Concepts, Air Force Office of Scientific Research, Avco-Everett Research Lab., Boston, MA, Oct. 1959: a) Sargent, W. H., and Gross, R. A., "A Detonation Wave Hypersonic Ramjet," Fairchild Engine Co.; b) Mager, A., and Baker, J., "On Efficient Utilization of Supersonic Combustion in Ramjets," Marquardt Aircraft; c) Dugger, G. L., Billig, F. S., and Avery, W. H., "Recent Work in Hypersonic Propulsion at the Applied Physics Laboratory, The Johns Hopkins University," Applied Physics Lab., TG-355, Johns Hopkins Univ., Nov. 1959; d) Weber, R. J., "Comments on Hypersonic Airbreathing Propulsion Papers," NASA Lewis Research Center.

[18]Selected Papers, National IAS-ARS Joint Meeting, Los Angeles,

CA, June 1961: *Advanced Air Breathing Propulsion*, a) Winter, J. S., and Drake, J. F., "Advanced Propulsion Systems for Aerospace Plane Applications," Marquardt Corp.; b) Dugger, G. L., Billig, F. S., and Avery, W. H., "Hypersonic Propulsion Studies at APL/JHU," Applied Physics Lab., Johns Hopkins Univ., Silver Spring, MD, TG-405, June 1961; c) Nau, R. A. (Convair), and Matsch, L. C. (Linde Co.), "Airborne Oxidizer Collection Systems"; d) Sens, W. H., Connors, V. W., and Slaiby, T. G., "Hydrogen Fueled Airbreathing Systems for Hypersonic Flight," Pratt & Whitney Aircraft; *Orbital Aircraft*, e) Bond, W. H., Fowler, R. G., Frick, C. W., Gay, A., and Mawhinney, R. F., "Analysis of Single-Stage-to-Orbit-Vehicles," Convair, Div. of General Dynamics; f) Kartveli, A., and Pappas, C. E., "Design Concepts and Technical Feasibility Studies of an Aerospace Plane," Republic Aviation Corp.

[19]Selected Papers, American Rocket Society 17th Annual Meeting and Space Flight Exposition, Los Angeles, CA, Nov. 1962: a) Eldredge, C. R., "Future Weapon Systems," Directorate of Research, Air Force; b) Schetz, J. A., "Diffusion and Combustion of Hydrogen in Air at Supersonic Speeds," General Applied Science Lab.; c) Krull, H. G., and Koffer, G. W., "Supersonic Combustion Research," Marquardt Corp.

[20]Weber, R. J., and MacKay, J. S., "An Analysis of Ramjet Engines Using Supersonic Combustion," NACA TN 4386, Sept. 1958.

[21]McLafferty, G. H., "Relative Thermodynamic Efficiency of Supersonic Combustion and Subsonic Combustion Hypersonic Ram jets," United Aircraft Rept. M-1351-3, East Hartford, CT, Oct. 1959.

[22]Roy, M., "Propulsion Supersonique par Turbonreacteurs et par Statoreacteurs," *Advances in Aeronautical Sciences*, Vol. 1, Pergamon, New York, 1959, pp. 79–112.

[23]Mordell, D. L., and Swithenbank, J., "Hypersonic Ramjets," *Second International Congress of the Aeronautical Sciences*, Pergamon, New York, 1960.

[24]Selected Papers, Fourth AGARD Colloquium, Combustion and Propulsion, High Mach Number Air Breathing Engines, Milan, Italy, April 1960, Pergamon, Oxford, England, UK, 1961: a) Ferri, A., "Possible Directions of Future Research in Air-Breathing Engines," General Applied Science Lab.; b) Zipkin, M. A., and Nucci, L. M., "Composite Air-Breathing Systems," General Electric and General Applied Science Lab.; c) Drake, J. A., "Hypersonic Ramjet Development," Marquardt Co.; d) Dugger, G. L., "Comparison of Hypersonic Ramjet Engines with Subsonic and Supersonic Combustion," Applied Physics Lab., Johns Hopkins Univ.; e) Behrens, H., and Roessler, F., "Supersonic Diffusion Flames," Institut Franco-Allemand de Recherches de Saint-Louis, France.

[25]Jamison, R. R., "Advanced Air Breathing Engines," Southampton Univ. Astronautics Seminar, Bristol Siddeley Engines Rept. T.R.H.58, Bristol, England, UK, July 1961.

[26]Kydd, P. H., and Mullaney, G. L., "Supersonic Combustion," *Combustion and Flame*, Vol. 5, Oct. 1961, pp. 315–318.

[27]Fowler, R. G., "A Theoretical Study of the Hydrogen-Air Reaction for Application to the Field of Supersonic Combustion," *Proceedings of the 1962 Heat Transfer and Fluid Mechanics Institute*, Stanford Univ. Press, 1962.

[28]Sreenath, A. V., "Studies of Turbo-Jet Engines for Hypersonic Propulsion," Mechanical Engineering Dept. Rept. SCS40, McGill Univ., Montreal, Canada, 1962.

[29]Libby, P. A., "Theoretical Analysis of Turbulent Mixing of Reactive Gases with Application to Supersonic Combustion of Hydrogen," *ARS Journal*, Vol. 32, No. 3, 1962, pp. 388–396.

[30]Lane, R.J., "Recoverable Air Breathing Booster for Space Vehicles," Royal Aeronautical Society Meeting, London, April 1962.

[31]Ferri, A., Libby, P. A., and Zakkay, V., "Theoretical and Experimental Investigation of Supersonic Combustion," Third International Congress of the Aeronautical Sciences, Stockholm, Sweden, Aug. 1962.

[32]Swithenbank, J., "Experimental Investigation of Hypersonic Ramjets," Third International Congress of the Aeronautical Sciences, Stockholm, Sweden, Aug. 1962.

[33]Burnett, D. R., and Czysz, P., "Supersonic Hydrogen Combustion Studies," Wright-Patterson AFB Rept. NR ASD-TDR-63-196, OH, April 1963.

[34]Curran, E. T., and Bergsten, M. B., "Discussion of Inlet Efficiency Parameters," Aeronautical Systems Div., ASRPR TM 62-68, Wright-Patterson AFB, OH, April 1963.

[35]Mestre, A., and Viaud, L., "Combustion Supersonique dans un Canal Cylindrique," 21st Meeting, AGARD Combustion and Propulsion Panel, London, April 1963.

[36]Pergament, H. S., "Theoretical Analysis of Non-Equilibrium Hydrogen-Air Reactions in Flow Problems," AIAA-ASME Hypersonic Ramjet Conf., Paper 63113, White Oak, MD, April 1963.

[37]Zakkay, V., and Krause, E., "Mixing Problems with Chemical Reactions," 21st Meeting, AGARD Combustion and Propulsion Panel, London, April 1963.

[38]Nicholls, J. A., Adamson, T. C., and Morrison, R. B., "Ignition Time Delay of Hydrogen-Oxygen-Diluent Mixtures at High Temperatures," *AIAA Journal*, Vol. 1, No. 10, 1963, pp. 2253–2257.

[39]Jeffs, R. A., and Beeton, A. B. P., "Liquid Air Cycle Engines for High Speed Aircraft," B.I.S. Aerospace Vehicles Symposium, Nov. 1963.

[40]Valenti, A. M., Molder, S., and Salter, G. R., "Gun-Launching Supersonic Combustion Ramjets," *Astronautics and Aerospace Engineering*, Vol. 1, No. 11, 1963, pp. 24–29.

[41]Schetz, J. A., "Supersonic Diffusion Flames," *Supersonic Flow, Chemical Processes and Radiative Transfers*, edited by D. B. Olfe and V. Zakkay, Pergamon, Oxford, England, UK, 1964, pp. 79–92.

[42]Swithenbank, J., "Design of the Hypersonic Aircraft," *Shell Aviation News*, No. 310, 1964, pp. 11, 12.

[43]Townend, L. H., and Reid, J., "Some Effects of Stable Combustion in Wakes Formed in a Supersonic Stream," *Supersonic Flow Chemical Processes and Radiative Transfer*, edited by D. B. Olfe and V. Zakkay, Pergamon, Oxford, England, UK, 1964, pp. 137–156.

[44]Franciscus, L. C., "Off Design Performance of Hypersonic Supersonic Combustion Ramjets," NASA TM X-52032, June 1964.

[45]Rhodes, R., "Research on Stabilized Normal Shock and Oblique-Shock Initiated Supersonic Combustion," USAFOSR Contractors Meeting, ARO, Tullahoma, TN, July 1964.

[46]Lindley, C. A., "Performance of Air Breathing and Rocket Engines for Hypervelocity Aircraft," International Council of the Aeronautical Sciences, AIAA Paper 64-557, Paris, Aug. 1964.

[47]Ferri, A., "Review of Problems in Application of Supersonic Combustion," Lanchester Memorial Lecture, Royal Aeronautical Society, London, May 1964; see also *Journal of the Royal Aeronautical Society*, Vol. 68, Sept. 1964, pp. 575–595.

[48]Dugger, G. L., and Monchick, L., "External Burning Ramjets, Preliminary Feasibility Study," Applied Physics Lab., CM 948, Johns Hopkins Univ., Laurel, MD, June 1959.

[49]Woolard, H. W., "An Approximate Analysis of the Two-Dimensional, Supersonic Flow Past a Plane Parallel Wall with Supercritical Heat Addition," Applied Physics Lab., CM 954, Johns Hopkins Univ., Laurel, MD, July 1957.

[50]Dugger, G. L., et al., "A Supersonic Combustion Ramjet Missile (SCRAM) for Naval Air Defense," Applied Physics Lab., TG-499, Johns Hopkins Univ., Laurel, MD, Sept. 1962.

[51]Dugger, G. L., Deklau, B., Billig, F. S., and Matthews, S. E., "Summary Report on External Ramjet Program," Applied Physics Lab., TG-419, Johns Hopkins Univ., Laurel, MD, Oct. 1961.

[52]Billig, F. S., "Current Problems in Nonequilibrium Gas Dynamics in Scramjet Engines," AIAA Professional Study Seminar on Nonequilibrium Gas Dynamics, Honolulu, HI, June 1987.

[53]Billig, F. S., "External Burning in Supersonic Streams," *Proceedings of the XVIIIth International Aeronautical Congress*, Belgrade, Yugoslavia, Sept. 1967, Pergamon, Oxford, England, UK, 1969, pp. 23–54.

[54]Billig, F. S., "Design and Development of Single-Stage-to-Orbit Vehicles," *Johns Hopkins APL Technical Digest*, Vol. 11, Nos. 3 and 4, 1990, pp. 336–352.

[55]Billig, F. S., and Van Wie, D. M., "Efficiency Parameters for Inlets Operating at Hypersonic Speeds," *Proceedings of the Eighth International Symposium on Air Breathing Engines*, Cincinnati, OH, June 1987, pp. 118–130.

[56]Waltrup, P. J., Anderson, G. Y., and Stull, F. D., "Supersonic Combustion Ramjet (Scramjet) Engine Development in the United States," Applied Physics Lab., Preprint Series 76-042, Johns Hopkins Univ., Laurel, MD, March 1976.

[57]Billig, F. S., Waltrup, P. J., and Stockbridge, R. D., "Integral-Rocket Dual-Combustion Ramjets: A New Propulsion Concept," *Journal of Spacecraft and Rockets*, Vol. 17, Sept.-Oct. 1980, p. 416–424.

[58]Billig, F. S., "Ramjets with Supersonic Combustion," AGARD-NATO PEP Lecture Series 136, Ramjet and Ramrocket Propulsion Systems for Missiles, London, Neubiberg, Germany, Sept. 1984, pp. 8-1–8-29.

[59]Billig, F. S., "Combustion Processes in Supersonic Flow," *Journal of Propulsion and Power*, Vol. 4, May–June 1988, pp. 209–216.

[60]Burnett, T. D., "Dual Mode Scramjet," Marquardt Corp., Air Force Aeropropulsion Lab., TR-67-132, Van Nuys, CA, June 1968.

[61]Harshman, D. L., "Design and Test of a Mach 7-8 Supersonic Combustion Ramjet Engine," AIAA Propulsion Specialist Meeting,

Washington, DC, July 1967.

[62]McLafferty, G.H., Krasnoff, E.L., Ranard, E.D., Rose, W.G., and Vergara, R.D., "Investigation of Turbojet Inlet Design Parameters," United Aircraft Corp. Research Dept. Rept. R-0790-13, East Hartford, CT, Dec. 1955.

[63]Waltrup, P. J., and Billig, F. S., "Structure of Shock Waves in Cylindrical Ducts," *AIAA Journal*, Vol. 11, No. 10, 1973, pp. 1404–1408.

[64]Carroll, B. F., and Dutton, J. C., "Characteristics of Multiple Shock Wave/Turbulent Boundary Layer Interactions in Rectangular Ducts," Dept. of Mechanical and Industrial Engineering, AIAA Paper 88-3805, Univ. of Illinois, Urbana, IL, July 1988.

[65]Billig, F. S., Corda, S., and Stockbridge, R. D., "Combustor-Inlet Interaction in Scramjet Engines," *APL Technical Review*, Vol. 2, No. 1, 1990, pp. 118–126.

[66]Hunter, L. G., and Couch, B. D., "A CFD Study of Precombustion Shock-Trains from Mach 3-6," AIAA/ASME/SAE/ASEE 26th Joint Propulsion Conf., AIAA Paper 90-2220, Orlando, FL, July 1990.

[67]Lin, P., Rao, G. V. R., and O'Connor, G. M., "Numerical Analysis of Normal Shock Train in a Constant Area Isolator," AIAA Paper 91-2162, June 1991.

[68]Stockbridge, R. D., "Experimental Investigation of Shock Wave/Boundary Layer Interactions in an Annular Duct," *Journal of Propulsion and Power*, Vol. 5, No. 3, 1989, pp. 346–352.

[69]Cohen, L. S., Coulter, L. J., and Egan, W. J., Jr., "Penetration and Mixing of Multiple Gas Jets Subjected to a Cross Flow," *AIAA Journal*, Vol. 9, No. 4, pp. 718–724.

[70]Cohen, L. S., Coulter, L. J., and Chiapetta, L., "Hydrocarbon-Fueled Scramjet," Supplement to Vol. VII *Tabulation of Data and Data Reduction Procedures for Fuel Distribution Investigation*, Air Force Aeropropulsion Lab., TR-68-146, U.S. Air Force, March 1970.

[71]Zukoski, E. E., and Spaid, F. W., "Secondary Injection of Gases into a Supersonic Flow," *AIAA Journal*, Vol. 2, No. 10, 1964, pp. 1689–1696.

[72]Spaid, F. W., Zukoski, E. E., and Rosen, R., "A Study of Secondary Injection of Gases into a Supersonic Flow," California Inst. of Technology, NASA TR 32-834, Pasadena, CA, Aug. 1966.

[73]Schetz, J. A., and Billig, F. S., "Penetration of Gaseous Jets Injected into a Supersonic Stream," *Journal of Spacecraft and Rockets*, Vol. 3, No. 11, 1966, pp. 1658–1665.

[74]Billig, F. S., Orth, R. C., and Lasky, M., "A Unified Analysis of Gaseous Jet Penetration," *AIAA Journal*, Vol. 9, No. 6, 1971, pp. 1048–1058.

[75]Orth, R. C., and Funk, J. A., "An Experimental and Comparative Study of Jet Penetration in Supersonic Flow," *Journal of Spacecraft and Rockets*, Vol. 4, No. 9, 1967, pp. 1236–1242.

[76]Schetz, J. A., Weinraub, R. A., and Mahaffey, R. E., Jr., "Supersonic Transverse Injection into a Supersonic Stream," *AIAA Journal*, Vol. 6, No. 5, 1988, pp. 933, 934.

[77]Chrans, L. J., and Collins, D. G., "Effect of Stagnation Temperature and Molecular Weight Variation of Gaseous Injection into a Supersonic Stream," *AIAA Journal*, Vol. 8, No. 2, 1970, pp. 287–293.

[78]Orth, R. C., Schetz, J. A., and Billig, F. S., "The Interaction and Penetration of Gaseous Jets in Supersonic Flow," NASA CR-1386, July 1969.

[79]Wu, J. M., and Aoyanna, K., "Analysis of Transverse Secondary Injection Penetration into Confined Supersonic Flow," AIAA Paper 69-2, New York, 1969.

[80]Adamson, T. C., Jr., and Nicholls, J. A., "On the Structure of Jets from Highly Underexpanded Nozzles into Still Air," *Journal of the Aerospace Sciences*, Vol. 26, No. 1, 1959, pp. 16–24.

[81]Love, E. S., and Grigsby, C. E., "Some Studies of Axisymmetric Free Jets Exhausting from Sonic and Supersonic Nozzles into Still Air and into Supersonic Streams," NACA RM L54L31, May 1955.

[82]Koch, L. N., and Collins, D. J., "The Effect of Varying Secondary Mach Number and Injection Angle on Secondary Gaseous Injection into a Supersonic Flow," AIAA Paper 70-552, May 1970.

[83]Povinelli, L. S., Povinelli, F. P., and Hersch, M., "A Study of Helium Penetration and Spreading in a Mach 2 Airstream Using a Delta Wing Injector," NASA TN D-5322, 1969.

[84]McClinton, C. R., "The Effect of Injection Angle on the Interaction Between Sonic Secondary Jets and a Supersonic Free Stream," NASA TN D-6669, Feb. 1972.

[85]Northam, G. B., Greenberg, I., and Byington, C. S., "Evaluation of Parallel Injector Configurations for Supersonic Combustion," AIAA Paper 89-2525, July 1989.

[86]Heister, S., and Karagozian, A., "The Gaseous Jet in Supersonic Crossflow," AIAA Paper 89-2547, July 1989.

[87]Marble, F. E., Zukoski, E. E., Jacobs, J. W., Hendricks, G. L., and Waitz, I. A., "Shock Enhancement and Control of Hypersonic Mixing and Combustion," AIAA Paper 90-1981, July 1990.

[88]Schetz, J. A., Thomas, R. H., and Billig, F. S., "Mixing of Transverse Jets and Wall Jets in Supersonic Flow," Separated Flows and Jets, International Union of Theoretical and Applied Mechanics Symposium, Novosibirsk, USSR, 1990, Springer-Verlag, Berlin, 1991.

[89]Wagner, J. P., Cameron, J. M., and Billig, F. S., "Penetration and Spreading of Transverse Jets of Hydrogen in a Mach 2.72 Airstream," NASA CR-1794, March 1971.

[90]King, P. S., Thomas, R. H., Schetz, J. A., and Billig, F. S., "Combined Tangential-Normal Injection into a Supersonic Flow," AIAA 27th Aerospace Sciences Meeting, AIAA Paper 89-0622, Reno, NV, Jan. 1989.

[91]Schetz, J. A., and Gilreath, H. E., "Tangential Slot Injection in Supersonic Flow," *AIAA Journal*, Vol. 5, No. 12, 1967, pp. 2149–2154.

[92]Walker, D. A., Campbell, R. L., and Schetz, J. A., "Turbulence Measurements for Slot Injection in Supersonic Flow," AIAA 26th Aerospace Sciences Meeting, AIAA Paper 88-0123, Reno, NV, Jan. 1988.

[93]Gilreath, H. E., and Sullins, G. A., "Investigation of the Mixing of Parallel Supersonic Streams," IX ISABE Meeting, Athens, Greece, Vol. 1, Sept. 1989, pp. 585–596.

[94]Bogdanoff, D. W., "Compressibility Effects in Turbulent Shear Layers," *AIAA Journal*, Vol. 21, No. 6, 1982, pp. 926, 927.

[95]Schadow, K. C., Gutmark, E., Koshigoe, S., and Wilson, K. J., "Combustion-Related Shear-Flow Dynamics in Elliptic Supersonic Jets," *AIAA Journal*, Vol. 27, No. 10, 1989, pp. 1347–1353.

[96]Papamoschou, D., and Roshko, A., "The Compressible Turbulent Shear Layer: An Experiment Study," *Journal of Fluid Mechanics*, Vol. 197, 1988, pp. 453–477.

[97]Schadow, K. C., Gutmark, E., and Wilson, K. J., "Passive Mixing Control in Supersonic Coaxial Jets at Different Convective Mach Numbers," AIAA 2nd Shear Flow Conf., AIAA Paper 89-0995, Phoenix, AZ, March 1989.

[98]Gutmark, E., Wilson K. J., Parr, T. P., and Hanson-Parr, D. M., "Combustion Enhancement in Supersonic Coaxial Flows," AIAA/ASME/SAE/ASEE 25th Joint Propulsion Conf., AIAA Paper 89-2788, Monterey, CA, July 1989.

[99]Gilreath, H. E., and Schetz, J. A., "Research on Turbulence in Hypersonic Engines," *APL Technical Review*, Vol. 2, No. 1, 1990, pp. 127–139.

[100]Sullins, G. A., Schetz, J. A., and Schadow, K. C., "Scramjet Mixing Studies," *APL Technical Review*, Vol. 2, No. 1, 1990, pp. 140–149.

[101]Schetz, J. A., and Billig, F. S., "Studies of Scramjet Flowfields," AIAA/SAE/ASME/ASEE 23rd Joint Propulsion Conf., AIAA Paper 87-2161, San Diego, CA, June–July, 1987.

[102]Schetz, J. A., Billig, F. S., and Favin, S., "Analysis of Slot Injection Beneath a Thick Hypersonic Boundary Layer," AIAA/ASME/SAE/ASEE 25th Joint Propulsion Conf., AIAA Paper 89-2457, Monterey, CA, July 1989.

[103]Schetz, J. A., Thomas, R. H., and Billig, F. S., "Gaseous Injection in High Speed Flow," *Ninth International Symposium on Airbreathing Engines*, Athens, Greece, AIAA, New York, Sept. 1989.

[104]Sherman, A., and Shetz, J., "Breakup of Liquid Sheets and Jets in a Supersonic Gas Stream," *AIAA Journal*, Vol. 9, No. 4, 1971, pp. 666–673.

[105]Schetz, J., Kush, E., and Joshi, P., "Wave Phenomena in Liquid Jet Breakup in a Supersonic Crossflow," *AIAA Journal*, Vol. 18, No. 7, 1980, pp. 774–778.

[106]Less, D., and Schetz, J., "Penetration and Breakup of Slurry Jets in a Supersonic Stream," *AIAA Journal*, Vol. 21, No. 7, 1983, pp. 1045, 1046.

[107]Forde, J., Molder, S., and Szpiro, J., "Secondary Liquid Injection into a Supersonic Airstream," *Journal of Spacecraft and Rockets*, Vol. 3, No. 8, 1966, pp. 1173–1176.

[108]Reichenbach, R., and Horn, K., "Investigation of Injectant Properties on Jet Penetration in a Supersonic Stream," *AIAA Journal*, Vol. 9, No. 3, 1971, pp. 469–472.

[109]Yates, C., and Rice, J., "Liquid Jet Penetration," Research and Development Programs Quarterly Rept., U-RQR/69-2, Applied Physics Lab., Johns Hopkins Univ., Laurel, MD, 1969.

[110]Catton, I., Hill, D., and MacRae, R., "Study of Liquid Jet Penetration in a Hypersonic Stream," *AIAA Journal*, Vol. 6, No. 11, 1968, pp. 2084–2089.

[111]Less, D. M., and Schetz, J. A., "Transient Behavior of Liquid

Jets Injected Normal to a High-Velocity Gas Stream," *AIAA Journal*, Vol. 24, No. 12, 1986, pp. 1979–1986.

[112]Hautman, D. J., and Rosfjord, T. J., "Transverse Liquid Injection Studies," AIAA Paper 90-1965, July 1990.

[113]Wilson, E., Jr., and Berl, W. G., "Fuels." Applied Physics Lab., TG 610-11, Johns Hopkins Univ., Laurel, MD, June 1974, Chap. 6.

[114]Kay, I. W., McVey, J. B., Kepler, C. E., and Chiappetta, L., "Hydrocarbon-Fueled Scramjet, Piloting and Flame Propagation Investigation," Air Force Wright Aeronautical Lab. TR-68-146, Wright-Patterson AFB, OH, Vol. IX, May 1971.

[115]Kay, I. W., Peschke, W. T., and Guile, R. N., "Hydrocarbon-Fueled Scramjet Combustor Investigation," AIAA Paper 90-2337, July 1990.

[116]Slack, M. W., "Rate Coefficient for $H + O_2 + M = HO_2 + M$ Evaluated from Shock Tube Measurements of Induction Times," *Combustion and Flame*, Vol. 28, No. 3, 1977, pp. 241–249.

[117]Bussing, T. R. A., and Eberhardt, S., "Chemistry Associated with Hypersonic Vehicles," AIAA Paper 87-1291, June 1987.

[118]Warnatz, J., "Concentration-, Pressure-, and Temperature-Dependence of the Flame Velocity in Hydrogen-Oxygen-Nitrogen Mixtures," *Combustion Science and Technology*, Vol. 26, Nos. 5 and 6, 1981, pp. 203–213.

[119]Hanson, R. K., and Salimian, S., "Survey of Rate Constants in the N/H/O System," *Combustion Chemistry*, edited by W. C. Gardiner Jr., Springer-Verlag, New York, 1984, Chap. 6, pp. 361–421.

[120]*Combustion Chemistry*, edited by W. C. Gardiner Jr., Springer-Verlag, New York.

[121]Brabbs, T. A., Lezberg, E. A., Bittker, D. A., and Robertson, T. F., "Hydrogen Oxidation Mechanism with Applications to (1) the Chaperon Efficiency of Carbon Dioxide and (2) Vitiated Air Testing," NASA TM 100186, Sept. 1987.

[122]Parthasarathy, K., and Zakkay, V., "An Experimental Investigation of Turbulent Slot Injection at Mach 6," *AIAA Journal*, Vol. 8, No. 7, 1970, pp. 1302–1307.

[123]Cary, A., and Hefner, J., "Film-Cooling Effectiveness and Skin Friction in Hypersonic Turbulent Flow," *AIAA Journal*, Vol. 10, No. 9, 1972, pp. 1188–1193.

[124]Hefner, J., and Cary, A., "Swept Slot Film Cooling Effectiveness in Hypersonic Turbulent Flow," *Journal of Spacecraft*, Vol. 11, No. 3, 1974, pp. 351, 352.

[125]Billig, F. S., and Grenleski, S. E., "Heat Transfer in Supersonic Combustion Processes," *Fourth International Heat Transfer Conference*, Heat Transfer 1970, Paris-Versailles, Aug. 1970, Vol. III, Elsevier, Amsterdam, 1970, FC 6.1 pp. 1–11.

[126]Billig, F. S., "Two-Dimensional Model for Thermal Compression," *Journal of Spacecraft and Rockets*, Vol. 9, No. 9, 1972, pp. 702, 703.

[127]Waltrup, P. J., Billig, F. S., and Stockbridge, E. S., "A Procedure for Optimizing the Design of Scramjet Engines," AIAA/SAE 14th Joint Propulsion Conf., AIAA Paper 78-1110, Las Vegas, NV, July 1978; see also *Journal of Spacecraft and Rockets*, Vol. 16, No. 3, 1979, pp. 163–172.

[128]Waltrup, P. J., Billig, F. S., and Evans, M.C., "Critical Considerations in the Design of Supersonic Combustion Ramjet (Scramjet) Engines," AIAA/SAE/ASME 16th Joint Propulsion Conf., AIAA Paper 80-1284, Hartford, CT, June 30–July 2, 1980; see also *Journal of Spacecraft and Rockets*, Vol. 18, No. 4, 1981, pp. 350–357.

[129]Schetz, J. A., Billig, F. S., and Favin, S., "Analysis of Mixing and Combustion in a Scramjet Combustor with Co-Axial Fuel Jet," AIAA/SAE/ASME 16th Joint Propulsion Conf., AIAA Paper 80-1256, Hartford, CT, June 1980.

[130]Schetz, J. A., Billig, F. S., and Favin, S., "Flowfield Analysis of a Scramjet Combustor with a Co-Axial Fuel Jet," *AIAA Journal*, Vol. 20, No. 9, 1982, pp. 1268–1274.

[131]Schetz, J. A., Billig, F. S., and Favin, S., "Scramjet Combustor Wall Boundary Layer Analysis," AIAA/SAE/ASME Joint Propulsion Conf., AIAA Paper 81-1434, Colorado Springs, CO, June 1981.

[132]Billig, F. S., White, M. E., and Van Wie, D. M., "Application of CAE and CFD Techniques to a Complete Tactical Missile Design," AIAA 22nd Aerospace Sciences Meeting, AIAA Paper 84-0387, Reno, NV, Jan. 9–12, 1984; see also "Numerical Methods for Engine-Airframe Integration," Vol. 102, Progress in Astronautics and Aeronautics, AIAA, New York, 1986, pp. 192–217.

[133]Schetz, J. A., Billig, F. S., and Favin, S., "Simplified Analysis of Scramjet Flowfields," *Journal of Propulsion and Power*, Vol. 4, No. 6, 1988, pp. 172–180.

[134]Schetz, J. A., Billig, F. S., and Favin, S., "Modular Analysis of Scramjet Flowfields," *Journal of Propulsion and Power*, Vol. 5, No. 2, 1989, pp. 172–180.

[135]Orth, R. C., Billig, F. S., and Grenleski, S. E., "Measurement Techniques for Supersonic Combustor Testing," *Instrumentation for Airbreathing Propulsion*, Symposium on Instrumentation for Airbreathing Propulsion, Vol. 34, Naval Postgraduate School, Monterey, CA, 1972, Progress in Astronautics and Aeronautics, AIAA, New York, Sept. 1972, pp. 263–282.

[136]Lee, R. L., Turner, R., and Billig, F. S., "Particulate Measurements in the APL Fuel-Rich Ramjet-Combustor Supersonic-Exhaust Flow," Western States Section/Combustion Inst., Pittsburgh, PA, Oct. 1980.

[137]Billig, F. S., Lee, R. L., and Waltrup, P. J., "Instrumentation for Supersonic Combustion Research," 1981 JANNAF Propulsion Meeting, New Orleans, LA; see also *CPIA Publication 340*, Vol. II, May 1981, pp. 67–100.

[138]Northam, G. B., Greenberg, I., and Byington, C. S., "Evaluation of Parallel Injector Configurations for Supersonic Combustion," AIAA Paper 89-2525, July 1989.

[139]Anderson, G. Y., and Gooderum, P. B., "Exploratory Tests of Two Strut Fuel Injectors for Supersonic Combustion," NASA TN-D-7581, 1974.

[140]Rogers, R. C., and Eggers, J. M., "Supersonic Combustion of Hydrogen Injected Perpendicular to a Ducted Vitiated Airstream," AIAA Paper 73-1322, Nov. 1973.

[141]Russin, W. R., "The Effect of Initial Flow Nonuniformity on Second-Stage Fuel Injection and Combustion in a Supersonic Duct," NASA TM X-72667, June 1975.

[142]Billig, F. S., Orth, R. C., and Funk, J. A., "Direct Connect Tests of a Hydrogen Fueled Supersonic Combustor," NASA CR-1904, Aug. 1971.

[143]Waltrup, P. J., and Billig, F. S., "Prediction of Precombustion Wall Pressure Distributions in Scramjet Engines," *Journal of Spacecraft and Rockets*, Vol. 10, No. 9, 1973, pp. 620–622.

[144]Billig, F. S., "Design of Supersonic Combustors Based on Pressure-Area Fields," *Proceedings of the Eleventh Symposium (International) on Combustion*, Combustion Inst., Pittsburgh, PA, 1967, pp. 755–769.

[145]Avrashkov, V., Baranovsky, S., and Levin, V., "Gasdynamic Features of Supersonic Kerosene Combustion in a Model Combustion Chamber," AIAA Paper 90-5268, Oct. 1990.

[146]"Hypersonic Research Engine Project Technological Status, 1971," NASA TM X-2572, Sept. 1972.

[147]"Hypersonic Research Engine Project—Phase II, Aerothermodynamic Integration Model Development—Final Technical Data Report," AP 75-11133, AiResearch Manufacturing Co. of California; NAS1-6666, NASA CR-132654, May 1975.

[148]Kepler, C. E., and Karanian, A. J., "Hydrogen-Fueled Variable-Geometry Scramjet," United Aircraft Research Lab., Air Force Aeropropulsion Lab., TR-67-150, East Hartford, CT, Jan. 1968.

[149]"Investigations of the Low Speed Fixed Geometry Supersonic Combustion Ramjet," General Applied Science Lab., Air Force Aeropropulsion Lab., TR-66-139, Westbury, NY, March 1967.

[150]Orth, R. C., and Erdos, J. I., "The Use of Pulse Facilities for Testing Supersonic Combustion Ramjet (SCRAMJET) Combustors in Simulated Hypersonic Flight Conditions," *Ninth International Symposium on Air Breathing Engines*, Vol. 1, Athens, Greece, Sept. 1989, pp. 596–604.

[151]Magar, A., "On the Model of the Free, Shock Separated Turbulent Boundary Taper," *Journal of the Aeronautical Sciences*, Vol. 23, No. 2, 1956, pp. 181–184.

[152]Crocco, L., "One Dimensional Treatment of Steady Gas Dynamic," *Fundamentals of Gas Dynamics, High Speed Aerodynamics and Jet Propulsion*, Vol. 3, Princeton Univ. Press, Princeton, NJ, 1958, pp. 105–130.

[153]Billig, F. S., "Scramjet Propulsion," Third Joint Europe/U.S. Short Course in Hypersonics, Aachen, Germany, Oct. 1990.

[154]Kumar, A., "Numerical Simulation of the Flow Through Scramjet Inlets Using a Three-Dimensional Navier-Stokes Code," AIAA Paper 85-1664, July 1985.

[155]Kumar, A., "Numerical Analysis of the Scramjet-Inlet by Using Two-Dimensional Navier-Stokes Equations," NASA TP-1940, Dec. 1981.

[156]Billig, F. S., and Grenleski, S. E., "Experimental Studies of Hydrogen-Air Ignition in a Supersonic Combustor," *Proceedings of the AIAA Second Propulsion Joint Specialists Conference*," Air Force System Command TR RTD TR-66-1, Vol. 1, Sept. 1966; see also Applied Physics Lab./Johns Hopkins Univ. TG 848, Laurel, MD, Aug. 1966.